

Light Water Reactor Sustainability Program

Status of the Flooding Fragility Testing Development

C. L. Pope, B. Savage, A. Sorensen, B. Bhandari, D. A. Kamerman, A. Tahhan, C. Muchmore, G. Roberts, E. Ryan, S. Suresh, A. Wells, C. Smith

June 2016

DOE Office of Nuclear Energy



DISCLAIMER

This information was prepared as an account of work sponsored by an agency of the U.S. Government. Neither the U.S. Government nor any agency thereof, nor any of their employees, makes any warranty, expressed or implied, or assumes any legal liability or responsibility for the accuracy, completeness, or usefulness, of any information, apparatus, product, or process disclosed, or represents that its use would not infringe privately owned rights. References herein to any specific commercial product, process, or service by trade name, trade mark, manufacturer, or otherwise, does not necessarily constitute or imply its endorsement, recommendation, or favoring by the U.S. Government or any agency thereof. The views and opinions of authors expressed herein do not necessarily state or reflect those of the U.S. Government or any agency thereof.

Light Water Reactor Sustainability Program

Status of the Flooding Fragility Testing Development

**C. L. Pope, B. Savage, A. Sorensen, B. Bhandari, D. Kamerman,
C. Muchmore, G. Roberts, E. Ryan, S. Suresh, A. Tahhan, A.
Wells – Idaho State University
C. Smith – Idaho National Laboratory**

June 2016

**Idaho National Laboratory
Idaho Falls, Idaho 83415**

<http://www.inl.gov/lwrs>

**Prepared for the
U.S. Department of Energy
Office of Nuclear Energy
Under DOE Idaho Operations Office
Contract DE-AC07-05ID14517**

ABSTRACT

This report provides an update on research addressing nuclear power plant component reliability under flooding conditions. The research includes use of the Component Flooding Evaluation Laboratory (CFEL) where individual components and component subassemblies will be tested to failure under various flooding conditions. The resulting component reliability data can then be incorporated with risk simulation strategies to provide a more thorough representation of overall plant risk.

The CFEL development strategy consists of four interleaved phases. Phase 1 addresses design and application of CFEL with water rise and water spray capabilities allowing testing of passive and active components including fully electrified components. Phase 2 addresses research into wave generation techniques followed by the design and addition of the wave generation capability to CFEL. Phase 3 addresses methodology development activities including small scale component testing, development of full scale component testing protocol, and simulation techniques including Smoothed Particle Hydrodynamic (SPH) based computer codes. Phase 4 involves full scale component testing including work on full scale component testing in a surrogate CFEL testing apparatus.

CONTENTS

ABSTRACT.....	iii
FIGURES.....	v
ACRONYMS.....	vi
1. INTRODUCTION.....	1
2. CFEL WATER RISE AND SPRAY DESIGN	3
3. CFEL WAVE IMPACT RESEARCH AND DESIGN	6
4. CFEL METHODOLOGY	14
4.1 Custom Validation Experiment.....	14
4.2 Flow Over Ogee Spillway Validation.....	16
5. FULL SCALE COMPONENT TESTING	27
6. CONCLUSION	33

FIGURES

Figure 1. CFEL research program roadmap.....	2
Figure 2. CFEL plan view.....	4
Figure 3. CFEL crane and reservoir elevation view.	5
Figure 4. CFEL storage and testing reservoir elevation view.....	5
Figure 5. Pressure distribution in the initial conditions for the solitary wave simulation.....	7
Figure 6. Pressure distribution of a solitary wave advancing forward on a beach.....	7
Figure 7. Velocity distribution of a solitary wave advancing forward on a beach.	8
Figure 8. Iso-view of pressures at imminent baffle impact.....	8
Figure 9. Wave impact simulation device design concept.....	10
Figure 10. WISD constant geometry design: wave section profile.....	10
Figure 11. WISD constant geometry design with standing water: wave section profile.	11
Figure 12. WISD constant geometry design with rotating plate: wave section profile.....	11
Figure 13. WISD partial contraction design concept.....	12
Figure 14. WISD partial contraction design concept: wave section profile.....	12
Figure 15. WISD syringe design concept.	13
Figure 16. WISD syringe design concept: wave section profile.....	13
Figure 17. Validation experiment apparatus.	15
Figure 18. Custom validation experiment photos.	15
Figure 19. Validation experiment measurements.....	16
Figure 20. Ogee dimensions and flow parameters.....	17
Figure 21. Horizontal flow particle emitter setup.	18
Figure 22. Bottom particle emitter setup.	18
Figure 23. Horizontal particle emitter wave beginning.	19
Figure 24. Horizontal particle emitter wave.	19
Figure 25. Horizontal particle emitter wave settled out.....	20
Figure 26. Splashing particles and emitted particles.....	20
Figure 27. Bottom particle emitter beginning.....	21
Figure 28. Bottom particle emitter with emitted particles.	21
Figure 29. Pressure tap locations.	22
Figure 30. Normalized discharge comparison.	22
Figure 31. Relative percent error in discharge using physical model as basis.....	23
Figure 32. Crest pressure comparison.....	24
Figure 33. Absolute pressure difference using physical model as baseline.....	25
Figure 34. Door failure in the Fukushima nuclear power plant.	27
Figure 35. Full-scale testing arrangement.....	28
Figure 36. Full-scale testing tank.....	29
Figure 37. Testing tank pressure relief valve, air vent, and pressure gauge.	29
Figure 38. Interior door installed in testing tank.....	30
Figure 39. Steel door example.....	31
Figure 40. Roll-Up door example.....	32

ACRONYMS

CFD	Computational Fluid Dynamics
CFEL	Component Flooding Evaluation Laboratory
NPP	Nuclear Power Plant
SPH	Smoothed Particle Hydrodynamic
WISD	Wave Impact Simulation Device

Status of the Flooding Fragility Testing Development

1. INTRODUCTION

The March 2011 tsunami at the Fukushima nuclear power plant (NPP) provided a reminder of the risk associated with flooding incidents in nuclear power plants. In addition, there have been flooding or near flooding events at other NPPs which have forced off-normal conditions and, in some cases, significant economic impacts. These flooding events highlight the need for improved and deeper understanding of the reliability of NPP components under flooding conditions. Improving NPP component reliability understanding will then support the ability to more accurately characterize the risk of such events.

To address this shortcoming, development of the Component Flooding Evaluation Laboratory (CFEL) is under way. In CFEL, individual components and component subassemblies will be tested to failure under various flooding conditions. These test results can then be used to develop component reliability models. Using the improved reliability models, improved risk modeling methodologies can be enhanced to allow a more thorough understanding of the NPP risks. These risk approaches are being investigated within the Department of Energy's Risk-Informed Safety Margins Characterization Pathway wherein we simulate complex scenarios such as internal or external plant floods.

CFEL will be capable of testing a variety of full scale NPP components to failure under water spray, water rise, and eventually wave impact flooding events. The mission of CFEL is a relatively novel undertaking. As such, the work scope has been divided into four interleaved tasks. The first two paths focus on installation of testing equipment to physically develop CFEL. The second two paths are research tasks that are proceeding in parallel with the laboratory installation and will mature as the laboratory becomes active.

The overall CFEL development strategy consists of four interleaved phases. Phase 1 addresses design and application of CFEL with water rise and water spray capabilities allowing testing of passive and active components including fully electrified components. Phase 2 addresses research into wave generation techniques followed by the design and installation of the wave generation capability. Phase 3 ensures full scale tests are wisely conducted by executing small scale component testing and developing full scale component testing protocol. Phase 4 involves full scale component testing including work on initial full scale component testing in a surrogate CFEL testing apparatus.

The laboratory installation has been divided into two phases with the goal of being able to naturally evolve the project from testing of simple components and scenarios to more complicated events with more prototypic components. The first phase focuses on the initial installation of CFEL and includes support for laboratory operation including modifications to the existing facility structures and electrical systems. In addition, it involves the installation of a crane for component handling tailored to handle components of interest, a below grade flooding chamber, and the expansion of the existing water reservoir. Everything required to conduct water rise and spray scenario testing will be installed as part of Phase 1. Phase 2 will focus on the modification of the facility to support dynamic wave impact testing. While the Phase 1 is underway, research is being conducted into wave impact event generation and simulation.

Programmatic research is being conducted in parallel with the CFEL design and consists of two 2 phases: the "Methodology Development and Small Scale Testing" Phase and the "NPP Component Testing" Phase. The former provides valuable insight into the direction of more complex tests and the latter provides the sustained capability to provide meaningful component reliability data. The program strategy for CFEL will be to begin with conducting a large number of simple tests using simple components consisting of existing or easy to

procure components and testing infrastructure. The goal of these lower rigor tests will be to develop a qualitative understanding of how different kinds of components such as structural, mechanical, and electrical components behave in various flooding scenarios and to better understand the uncertainties behind failures. The concept of damage states corresponding to different cross sectional areas of the doorway is an example of a qualitative conclusion which was observed while observing a small scale door failure test. This task will seek to discover similar observations and apply new and creative stochastic models that describe the failure of components based on the results of actual testing. These test results can then be used to improve risk models involving flooding events where doorways play a significant role in determining the overall risk.

As the CFEL capability expands, the testing methodology and sophistication will increase, building on the experience gained in early testing. Testing with actual NPP components will carry costs and the testing protocol must be highly refined prior to conducting these tests to ensure the quality of the data is sufficient for use in assessing NPP risks.

Figure 1 shows the integrated roadmap for the CFEL research program. Greater detail is provided for those activities taking place in the near term while goals for longer term research are identified as it is recognized that the roadmap for CFEL will need to evolve as the laboratory is installed, data is collected, and stakeholder input is obtained. This strategy provides a roadmap with defined goals and a logical approach while also remaining adaptable to evolving as lessons are learned over time.

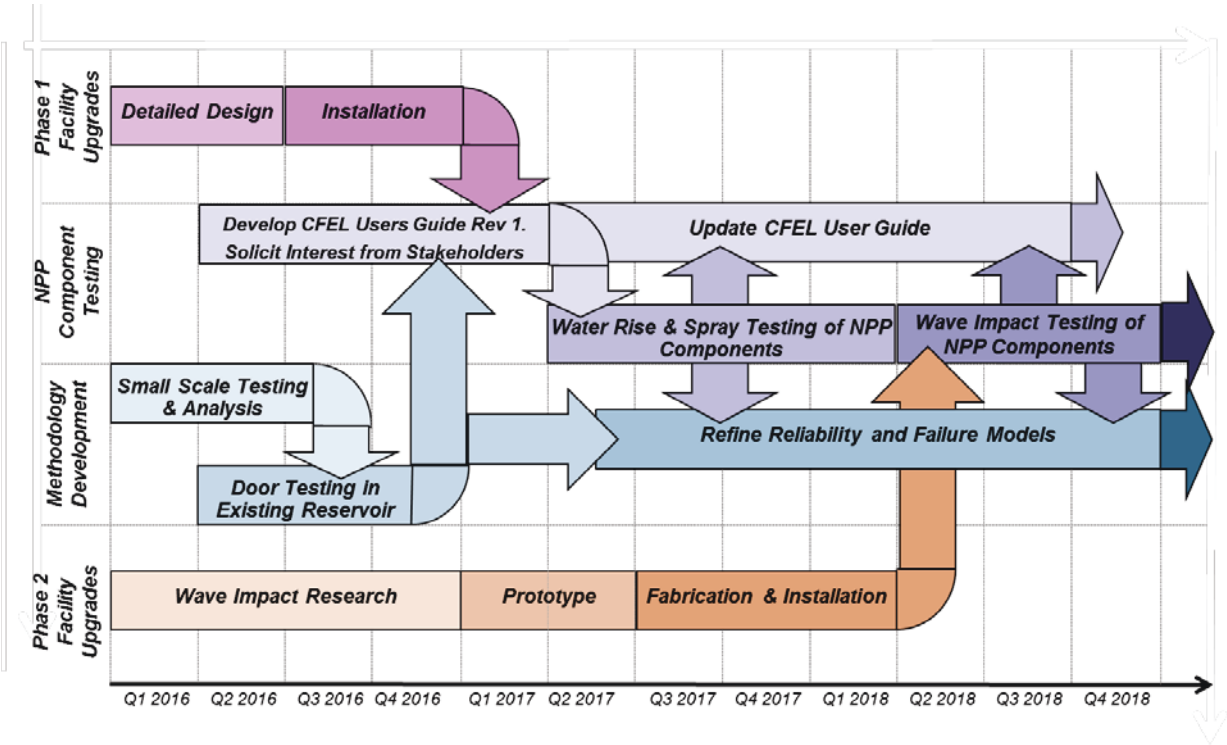


Figure 1. CFEL research program roadmap.

2. CFEL WATER RISE AND SPRAY DESIGN

CFEL will occupy a currently unused space in the laboratory that is 24 feet in width and 70 feet long. A large roll-up door adds to the appeal, as it will support easy receipt of components. The facility will include a water storage capacity of approximately 36,000 gallons. The water storage capacity will consist of an existing 8,000-gallon below grade water reservoir, a new 23,000-gallon below grade water reservoir, and a new 5,000-gallon below grade culvert connecting the existing and new reservoirs.

Like the storage reservoirs, the component testing bay is also located below grade. The testing bay will be 22.5 ft long, 12 ft wide, and 12 ft deep. The useable volume of the testing bay is approximately 20,000 gallons. The testing bay will include a removable cover to allow experiments that involve simulation of water depths up to 40 feet. An overhead crane will also allow component installation and removal. Initial engineering drawings of the CFEL facility are provided in Figure 2, Figure 3, and Figure 4.

To accommodate the variety of components desired for experimentation at CFEL an overhead crane will need to be installed into the CFEL. Components for testing will enter the laboratory via the rollup door. The components will then likely need to be moved to a staging area and eventually loaded into the testing bay. Following the destruction of the component in the testing chamber it will again need to be removed for examination and eventual removal from the facility. Initial scoping has indicated that a 5-ton capacity crane would be ideal for most components that would be tested.

One of the main types of components that are desired for testing is electrical components. As these components will be tested live, it will be necessary for them to be isolated from the balance of the building electrical supply such that when the components fail they do not cause facility wide outages.

Core drilling of the reservoir area was conducted June 3, 2016. Initial indications are that there are no excavation interferences. A design concept review was conducted June 24, 2016 and concept approval was granted. Engineering design development is now underway and is expected to finish in July. Preparation of construction documents will then occur followed by construction bidding. Construction is anticipated to begin in the Fall and completion is expected to finish in early 2017.

Flood testing in CFEL will take on a variety of different forms. The water rise rates in the tank are likely to be a critical variable in understanding how the components fail. As such it may be desirable to be able to segment the flooding chamber into smaller sections to produce a higher rate of water rise for a given flowrate. For the spray testing and later wave impact testing, large volumes of high velocity water will impact the sides of the flooding chamber. As such the chamber will be required to have walls that are capable of bearing these heavy loads and be resistant to degradation from the high velocity water jets.

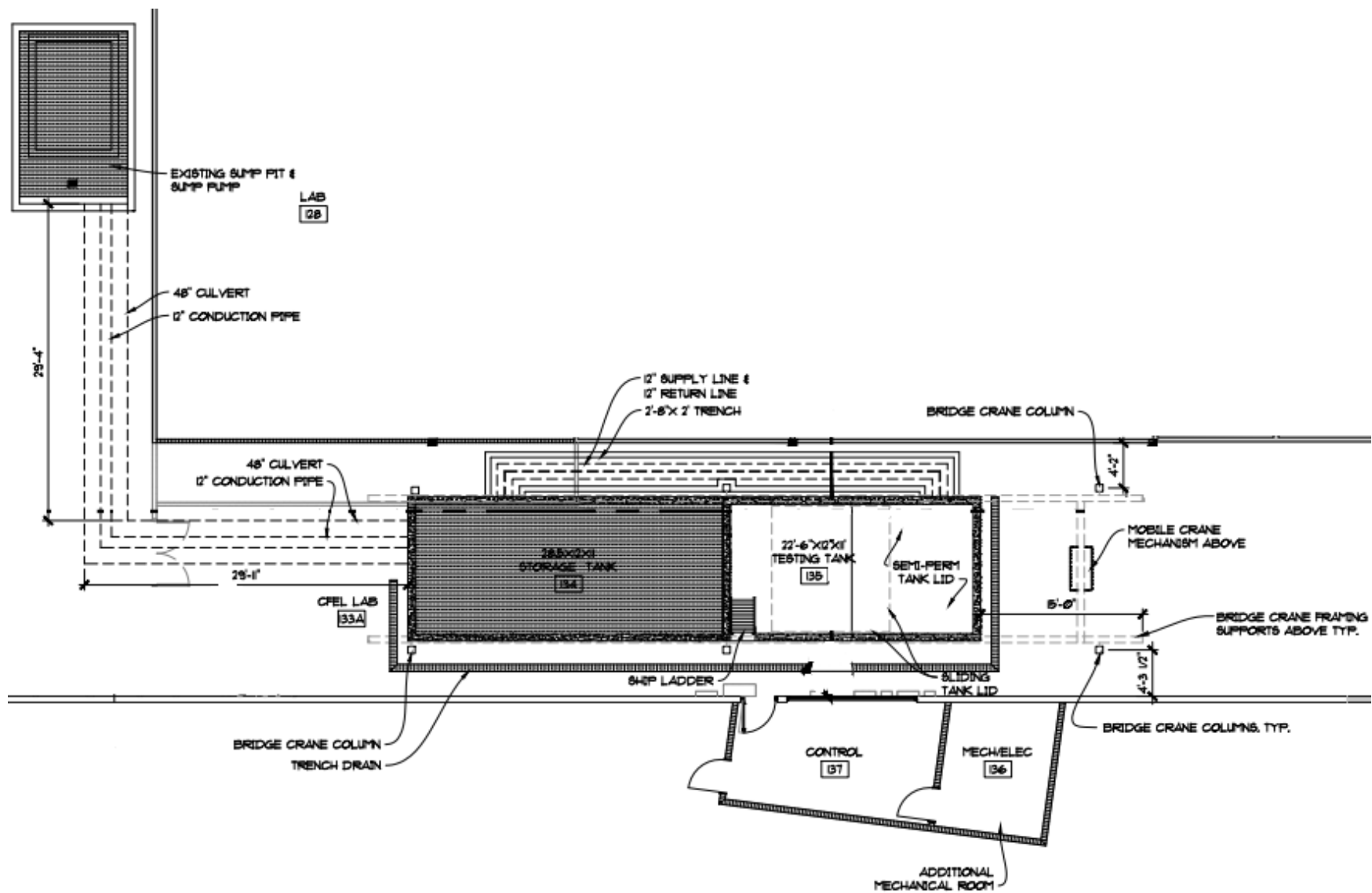


Figure 2. CFEL plan view.

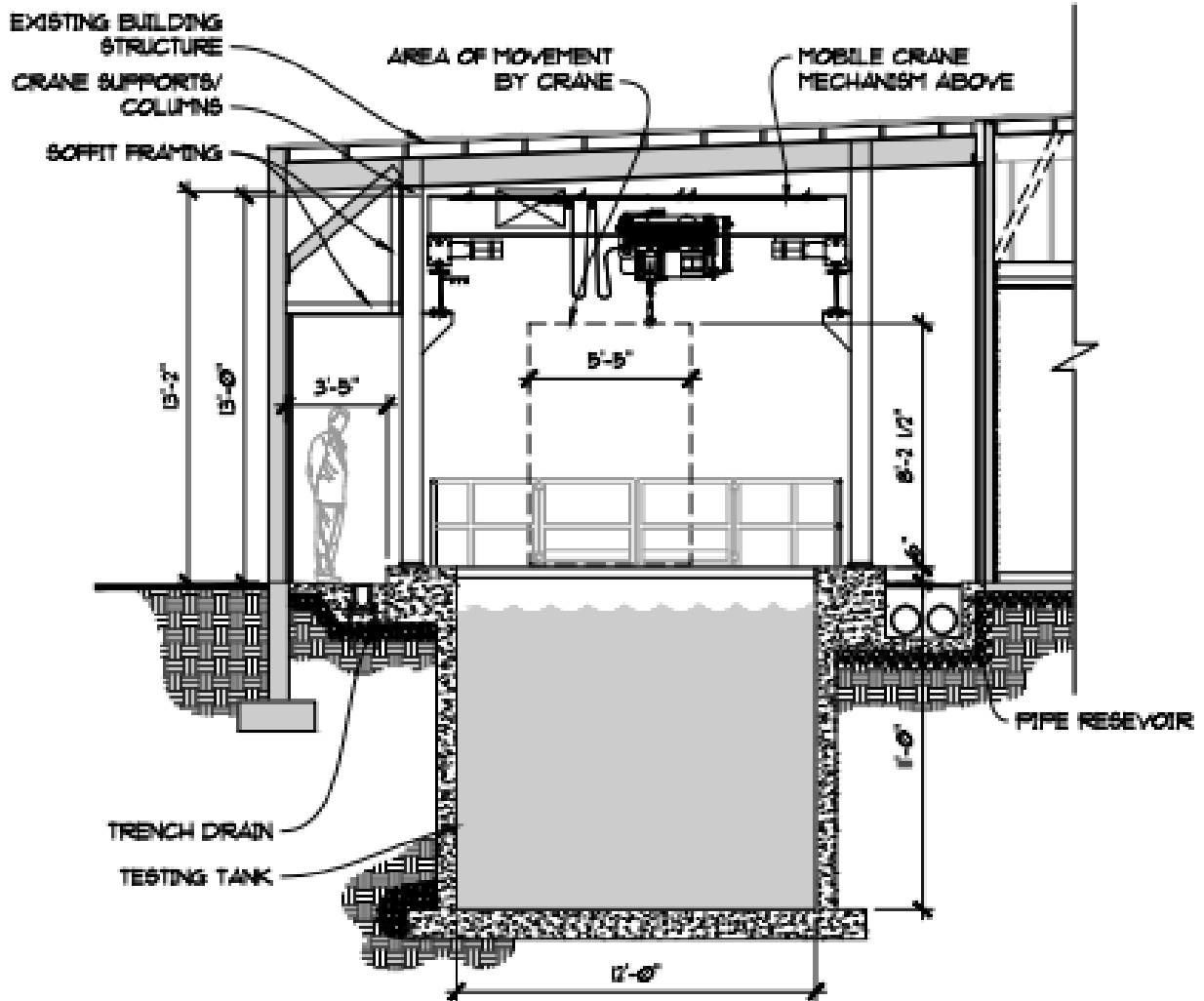


Figure 3. CFEL crane and reservoir elevation view.

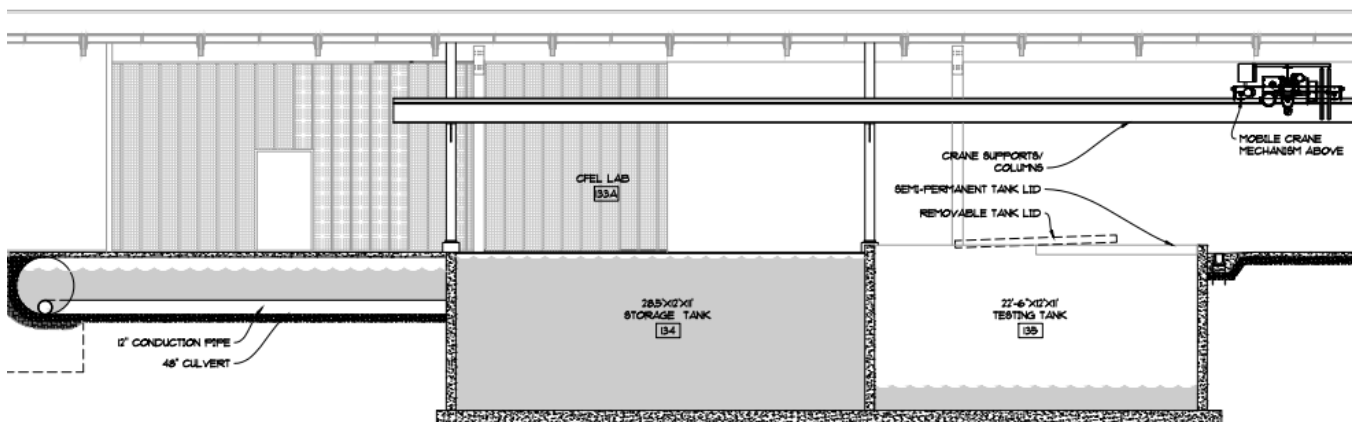


Figure 4. CFEL storage and testing reservoir elevation view.

3. CFEL WAVE IMPACT RESEARCH AND DESIGN

The CFEL facility design described above is specifically arranged to accommodate wave impact generation equipment. The accommodation includes maximization of the water storage capacity, robust testing bay concrete to resist debris and wave impacts, and reserving sufficient space in an easy to access area for the eventual installation of the wave generation equipment.

The continuing objective of the CFEL Phase 2 is the conceptual development of a wave generator that can test the effect of large waves, up to 20 feet, impacting on different prototype components. The project primary focus is to model tsunami waves and their impacts, but other extreme wave events such as storm surges or a dam break could be included as well. Since the development of a wave generation device that can generate a 20-foot wave would be economically prohibitive, efforts have been directed towards creating a wave impact simulation device (WISD) that can create a section of a wave that replicates the forces seen in the tsunami wave simulations.

Initial efforts focused on reviewing existing wave generation devices and wave mechanics. The literature shows that tsunamis are modeled using scaled models with solitary waves or N-waves, and wave generation in physical models are accomplished by using a moving paddle or plunger.^{1 2} It was also noted that the wave geometry is a function of approach geometry (slope/depth), angle of approach and wave generation. However, the maximum velocity of a wave is limited by critical flow; defined by a Froude number equal to one. The Froude number is used in free surface flows to define the flow regime as subcritical, critical or supercritical.³ In simple terms, the Froude number defines the speed of sound (or celerity wave) in water similar to the way that the Mach number defines the speed of sound in air. Velocities greater than the speed of sound are classified as supersonic, and velocities less than the speed of sound are called subsonic. At a Mach number equal to one, the flow is considered sonic. However, it should be noted that wave mechanics are not simple. Waves are classified as deep or shallow waves based on wavelength and fluid depth. Deep water wave speed is independent of the depth, but shallow water wave speed is a function of the depth. Maximum wave velocity is based on a ratio of the wavelength versus the fluid depth, and for shallow waves, the maximum wave velocity is limited to a Froude number of one.⁴ Since tsunami waves have enormous wavelengths, they behave as shallow waves, even in deep water. Therefore, to create a section of a wave that will match the wave impact force over a defined area, the velocity tied to Froude number of 1 will be used. Equation 1 shows the general Froude equation for shallow water waves:

$$v = \sqrt{gD} \quad (1)$$

where v is the velocity (ft/s), g is gravitational acceleration (32.2 ft/s²), and D is the wave depth (ft).

Solitary waves are modeled with computational fluid dynamics (CFD) simulating tsunami waves with a height of 20 feet. The model provides flow data such as peak impact forces, pressures and velocities from the

¹ Malek-Mohammadi, S. and Testik, F. "New Methodology for Laboratory Generation of Solitary Waves." *Journal of Waterway, Port, Coastal, and Ocean Engineering*, Vol. 136(5), 286–294, 2010.

² Goseberg, N., Wurpts, A., and Schlurmann, T. "Laboratory-scale generation of tsunami and long waves." *Coastal Engineering*, Vol. 79, 57-74, 2013.

³ Akan, A. Osman. "Open Channel Hydraulics." Burlington, MA: Elsevier; Butterworth-Heinemann, 2006.

⁴ Mayo, N. "Ocean Waves-Their Energy and Power." *Physics Teacher* 35, 352, Sept. 1997.

simulations. This information is used as design input for the WISD. The commercial code Flow-3D by Flow Science is well known for its ability to track free surface flows.

Using Flow-3D, the 20-foot tsunami waves are simulated as solitary waves, and the impact forces caused by the waves are recorded for a chosen approach geometry. In each simulation, the 20-foot high solitary wave travels from left to right in a body of water with a constant 20 foot depth, and approaches a ten degree slope leading to a horizontal beach. To reduce computational time, the simulations are designed as sectional models; a thin slice of an infinitely wide wave perpendicularly approaching a shoreline. This effectively creates a 2D model that is valid because the flow variations parallel with the beach are not significant. Figure 5 shows the initial velocity conditions of the wave simulation at time zero, and Figure 6 and Figure 7 display the pressure and velocity patterns of the wave as it travels from left to right towards the horizontal beach. The impact force on a small baffle located on the beach at various locations provides insight into how a wave impacts structures and the effective force of the wave based on what height of the wave impacts the component (baffle) first. A baffle about to be struck by the solitary wave is shown in Figure 8. Impact forces at various locations and elevations are recorded in the horizontal beach zone. Figure 6 shows that the wave front moves forward with an atmospheric pressure.

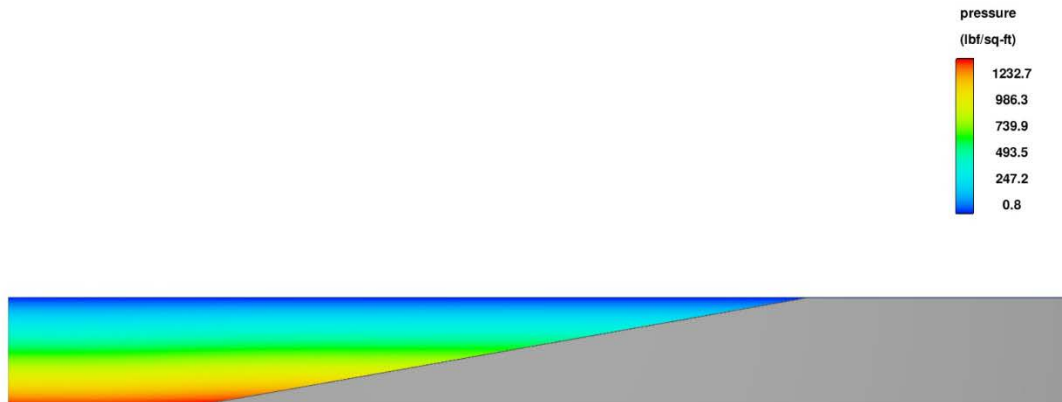


Figure 5. Pressure distribution in the initial conditions for the solitary wave simulation.

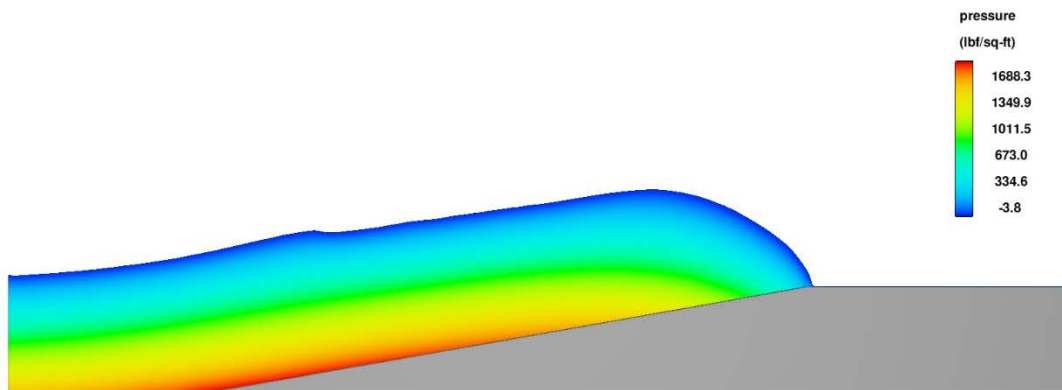


Figure 6. Pressure distribution of a solitary wave advancing forward on a beach.

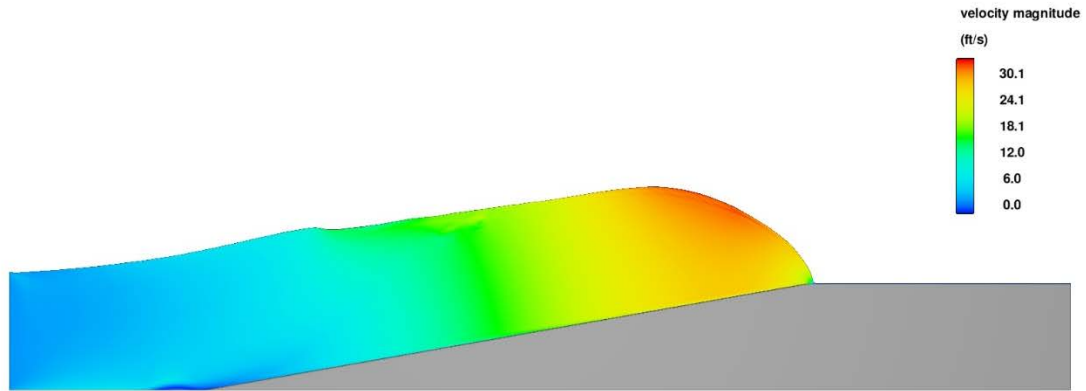


Figure 7. Velocity distribution of a solitary wave advancing forward on a beach.

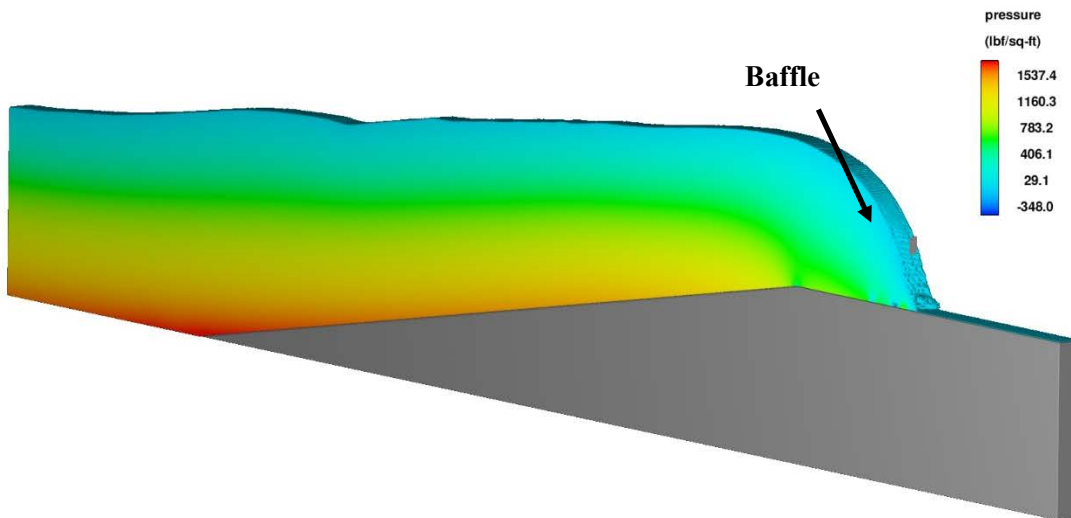


Figure 8. Iso-view of pressures at imminent baffle impact.

Defining a tsunami wave as a shallow water wave as it approaches the shoreline, Equation 1 gives a velocity of 25.4 feet per second for a wave height of 20 feet. This is the target velocity in the development of the WISD. To create a velocity of this magnitude over a short distance, the concept of a plunger or syringe was developed. Similar to other wave generating devices, the motion of the water would be initiated by a paddle or plunger either pushing the water forward or pushing it down and translating the increased pressure into forward motion. This would in effect create a large jet that would impact the object of interest with the same velocity as a wave. The jet would exit the tube/nozzle prior to impact, allowing the atmospheric pressure to be developed at the face of the jet. The jet area would be large enough to completely surround the target, modeling a wave that is larger than the target on either side and above it. Assuming that test objects such as double doors could be 6 feet high by 7 feet wide, the initial jet size was fixed at 10 feet wide by 10 feet high, providing sufficient area on either side of door when the modified wave/jet impacts the area.

A simple calculation can be performed using the impulse momentum equation to quantify the amount of energy required to force a fluid mass to undergo a sudden change in velocity. The impulse momentum equation used for a simplified energy calculation is given below:

$$F = \frac{m\Delta V}{\Delta t} \quad (2)$$

where F is force (lb), Δt is the change in time (s), m is the fluid mass (lb·s²/ft), and ΔV is the change in velocity (25.4 ft/s).

The force required to cause a 1000 cubic foot mass of water to go from an initial velocity of zero to a final velocity of 25.4 feet per second can be calculated. The mass of the fluid is calculated by multiplying the mass of water, 1.94 slugs per cubic foot, by the fluid volume, 1000 cubic feet. To determine the change in time, the target velocity of 25.4 feet per second is used, along with an assumed distance of ten feet, an assumed conduit length. Dividing the assumed distance by the target velocity gives a change in time of approximately 0.39 seconds. Using these values, the required force is calculated to be approximately 126,350 pounds, or approximately 63.2 tons. This calculation shows that an enormous amount of energy is required to rapidly displace a large fluid volume. If the time is decreased so that a constant velocity is reached quicker and the flow field is allowed to stabilize prior to impact, the required force will be larger.

Since creating a 20-foot wave in a laboratory is not feasible, different models have been simulated in Flow-3D to determine an ideal design for a WISD capable of creating a near vertical section that will match the impact forces of a 20-foot wave. Different models have explored hinged paddles, vertical plungers such as a large concrete block and horizontal plungers/rams. Current configurations are exploring additional options with the closed conduit systems utilizing horizontal rams to create this wave section. One problem that has been identified in the modeling is that the gravitational acceleration across the 10-foot vertical height is sufficient to pull the water down towards the base, creating a sloping face or a tongue to the advancing jet. Although in traditional waves a small advance front or tongue may be present, the sloping of the wave face is minimized by the wave moving over relatively still water that has to be entrained due to momentum transfer. The wave is impeded as it moves up a sloping beach and moves over and past large scale roughness such as shrubs/trees, rocks/boulders or man-made objects. In the short prototype channel, there is nothing to impede the water flow to prevent the tongue from developing and minimizing the sloping front. Figure 9 shows a cross-section of a system that is being simulated in an effort to reduce the sloping front. A vertical plate, shown in black, pushes the water from right to left at a velocity of 25.4 feet per second into a test pit, where an object can be subjected to impact testing. A shallow basin of water is placed at the conduit exit to slow any water at the base of the wave that enters the test pit before the wave section.

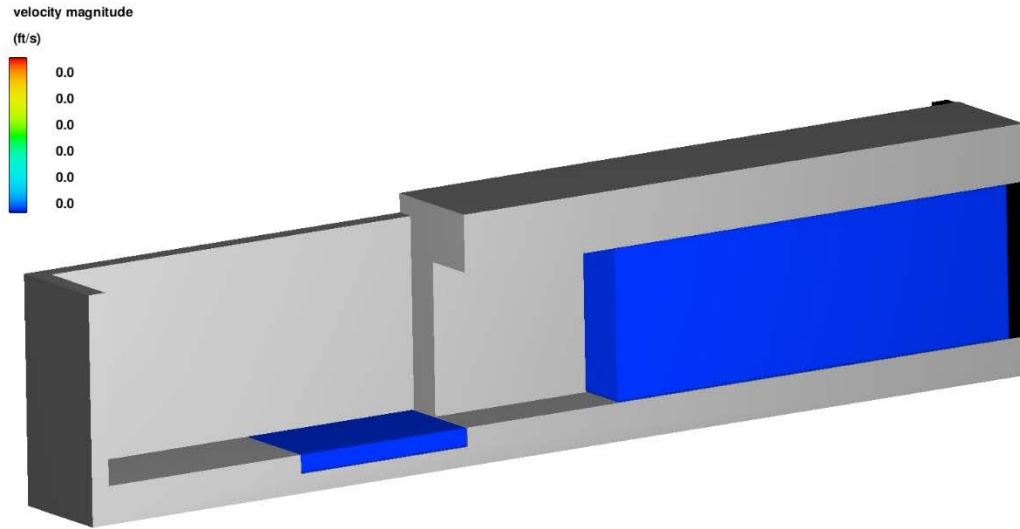


Figure 9. Wave impact simulation device design concept.

Figure 10 shows the advancing wave front just prior to reaching the basin of water. Although the majority of the sloping face is moving at the correct velocity, the velocity at the base of the jet has increased and the top of the jet has decreased due to the gravitational acceleration. When the advancing wave reached the basin, it skimmed over the water, doing little to reduce the advancing front.

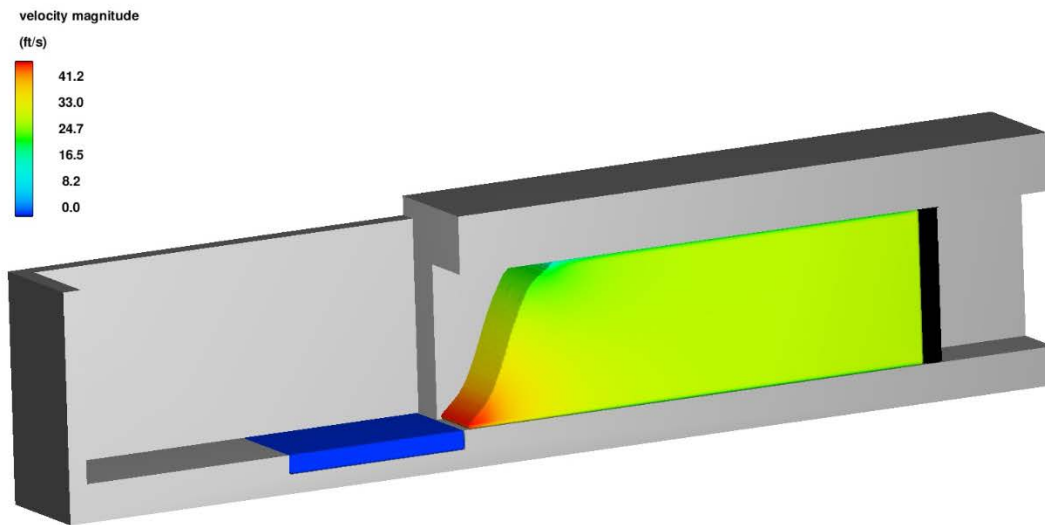


Figure 10. WISD constant geometry design: wave section profile.

Additional geometries are being investigated in an effort to improve the wave front. Figure 11 shows the effect of placing a layer of water inside the jet conduit to impede the advancing flow at the start. As shown in the figure, the additional water does reduce the run-out in front and starts to develop a vertical wave face that intersects with the falling fluid, moving the tongue vertically higher. Although it has not been simulated yet, it is believed that if the conduit was longer and there was sufficient water to entrain, the tongue would continue to be moved upward until the entraining water was pushed to the conduit ceiling, creating a more realistic conditions

for wave impact tests. However, a longer conduit would also require the pushing rams to continue a farther distance.

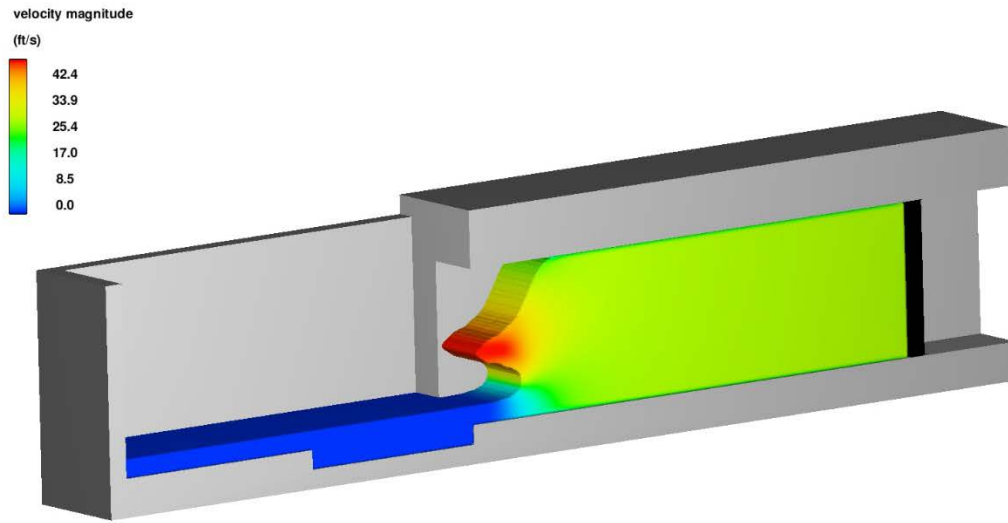


Figure 11. WISD constant geometry design with standing water: wave section profile.

The constant geometry design is again modified by specifying plate rotation. By rotating the plate counterclockwise and then moving it horizontally, the fluid near the top of the conduit is accelerated in an attempt to match the fluid velocity at the base of the wave section. As shown by Figure 12, the wave section has a more vertical profile using this approach, but a tongue of water still forms at the base of the wave ahead of the wave section.

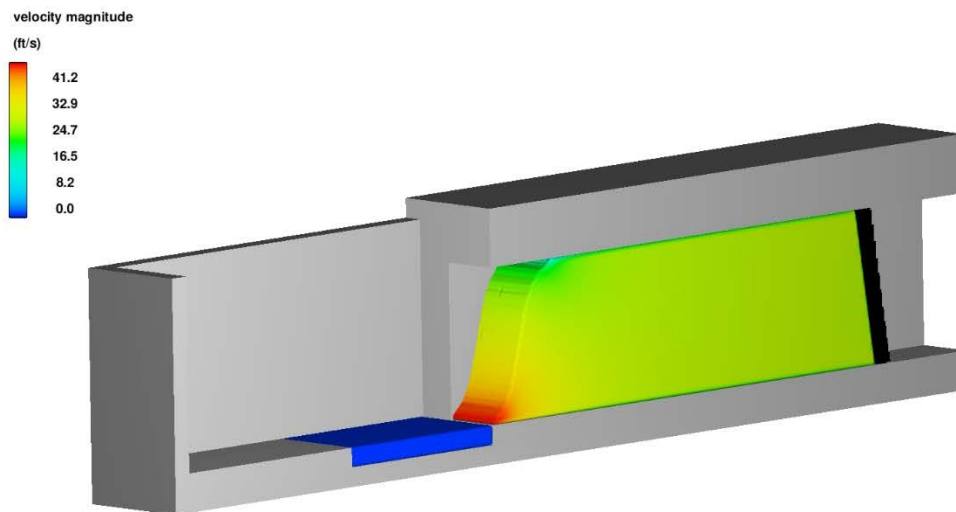


Figure 12. WISD constant geometry design with rotating plate: wave section profile.

A design with a contraction at the top of the wave tank to accelerate the fluid entering the conduit is also being investigated. Figure 13 shows this simulation at time zero. As the vertical plate pushes water out of the wave tank, a near vertical wave face is formed as the water exits the conduit, as seen in Figure 14. The tongue at the base of the wave is reduced, and the most promising result is yielded by this approach. It is noted, however, that due to the contraction, velocities greater than the target 25.4 feet per second are produced as the fluid exits

the conduit. By reducing the velocity of the plate, the velocity of the fluid exiting the conduit will converge to the desired value, but this change may lead to a more sloped wave section. Simulations will be run with a reduced plate velocity to observe the behavior of the wave face.

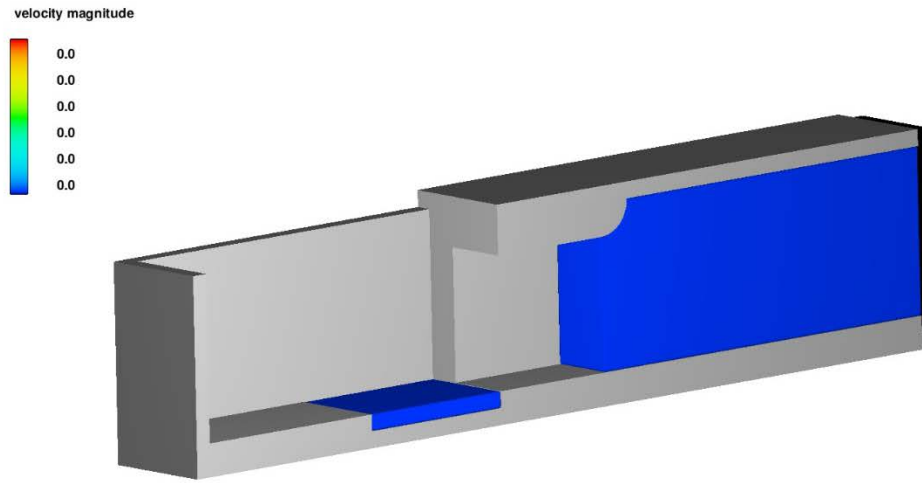


Figure 13. WISD partial contraction design concept.

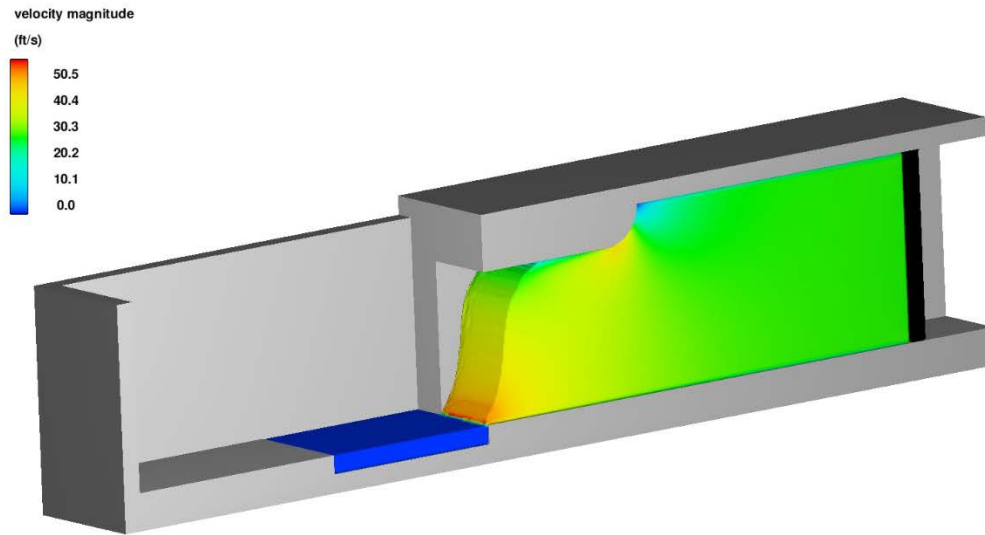


Figure 14. WISD partial contraction design concept: wave section profile.

Finally, a design based on the concept of a syringe is being considered. The top of the tank and the sides use fillets to form a contraction into the conduit. The vertical plate pushes water out of the wave tank into the narrowing conduit, and the fluid then exits the conduit into the test pit. Figure 15 shows the system at time zero. The contractions on the top and sides of the tank do little to help form a near vertical wave face as shown in Figure 16.

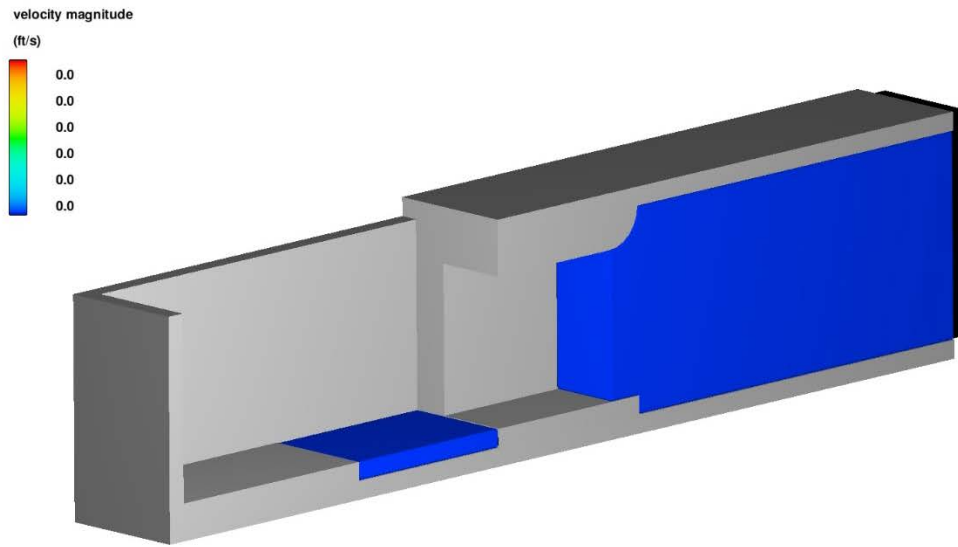


Figure 15. WISD syringe design concept.

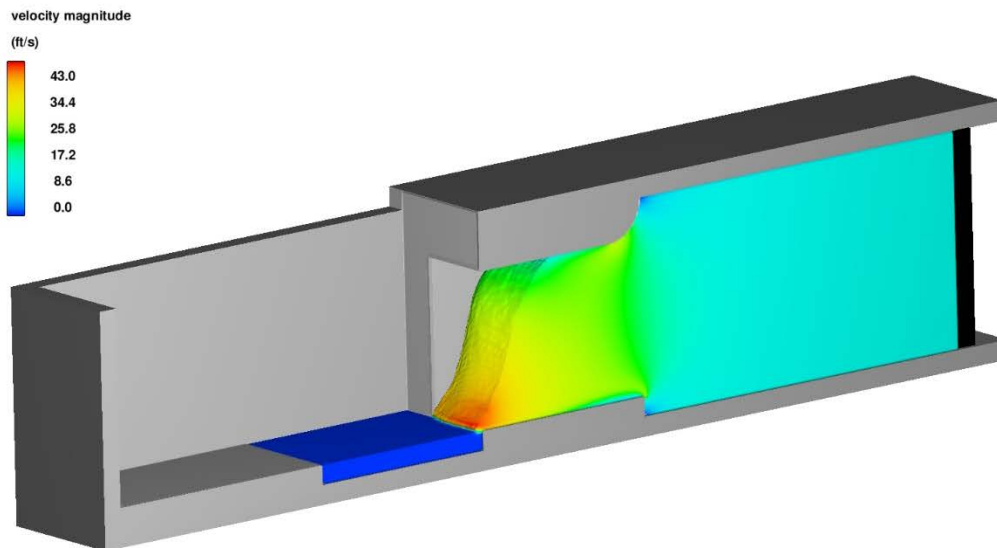


Figure 16. WISD syringe design concept: wave section profile.

Many concepts are being investigated for the WISD. As more information is drawn from these investigations, several of the most promising designs will be pursued with the goal of developing a prototype WISD to utilize in Phase 2 portion of the project. The results from the prototype testing will then determine the design chosen for the full scale WISD for CFEL.

4. CFEL METHODOLOGY

Smoothed Particle Hydrodynamics (SPH) has been investigated for modeling and simulating flooding scenarios. Previous work was done to identify different SPH codes and determine which codes would merit further investigation. The investigation included installing the code, running the code, and examining the code output. From this work, two codes were chosen for further investigation: DualSPHysics and GPUSPH. Both codes are open source codes. After the initial identification of SPH codes, two additional codes were identified and are also of interest: Neutrino, which is proprietary, and LAMMPS, which is open source.

Since four codes have been identified for further investigation, the next step is to validate these codes with unique and different validation cases. Most of these codes have been validated by using a set of default validation cases. However, in order to determine if the code is capable of modeling a flooding scenario accurately, a different and unique validation case needs to be conducted. The next section will discuss the validation cases that will be used for validating the SPH codes.

Validation is an essential part of any code. It allows the users to know that the results from the code can be trusted and match the physical system they are modeling. Therefore, validation is a crucial part in determining what SPH codes should continue to be looked at and what codes do not provide realistic behaviors. Two validation cases have been chosen to be used for the validation of the SPH codes. One is a custom experiment and the other is a known CFD validation. The next sections will detail these validation cases.

4.1 Custom Validation Experiment

A custom experiment was chosen as a validation case for all four of the SPH codes. The custom experiment consists of water flowing, by gravity, into a 3D printed box. Inside this box is another smaller box. Water will flow into the smaller box once it has reached a certain level. With this experiment, the water level and water flow rate are able to be monitored as well as the time when the water starts to overflow into the small box. This information will then be compared to the SPH simulations and will allow for validation of these codes. This validation case will be modeled in all four codes since it is a simple gravity fed water tank.

The validation work is taking place in three steps. The first step is the experiment. A more detailed explanation of the experiment is provided below. The second step consists of solving the problem analytically. This step uses the Bernoulli equation and conservation of mass to develop two differential equations that can be solved to develop an equation that will relate the time after the start of the test to the height of the water in the inner box. The final step is modeling the experiment in the SPH code of choice, in order to replicate the results obtained from the previous two steps.

Figure 17 shows the setup of the experiment. The experiment consists of a cylinder (1) filled with water above a box (2). The box has a smaller box in the center (3) of it that is shorter than the sides of the outside box. Water flows through a hole in the bottom of the cylinder and fills the volume around the outer box. The water then crests the inner box and partially fills it. The height of the water over time in the center box is measured with an ultrasonic sensor (4). Additionally, video is recorded of the experiment to compare to the SPH codes as another measure of validation other than the height measurements from the sensor. To aid the visibility of the water in the video, a small amount of dye is added. Figure 18 shows photos of the experiment process with the graduated cylinder filled, draining, and the final state of the experiment.

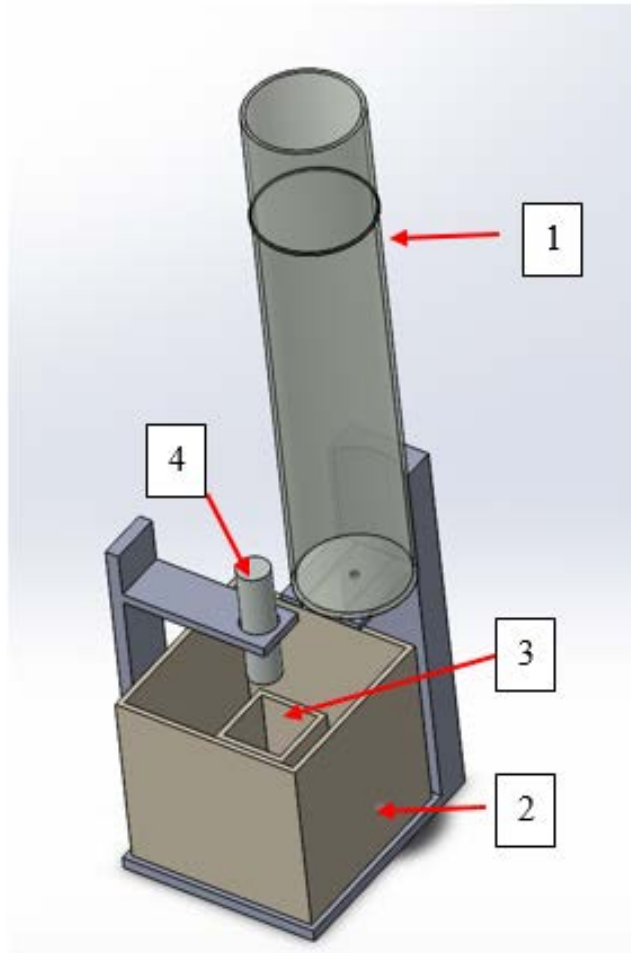


Figure 17. Validation experiment apparatus.

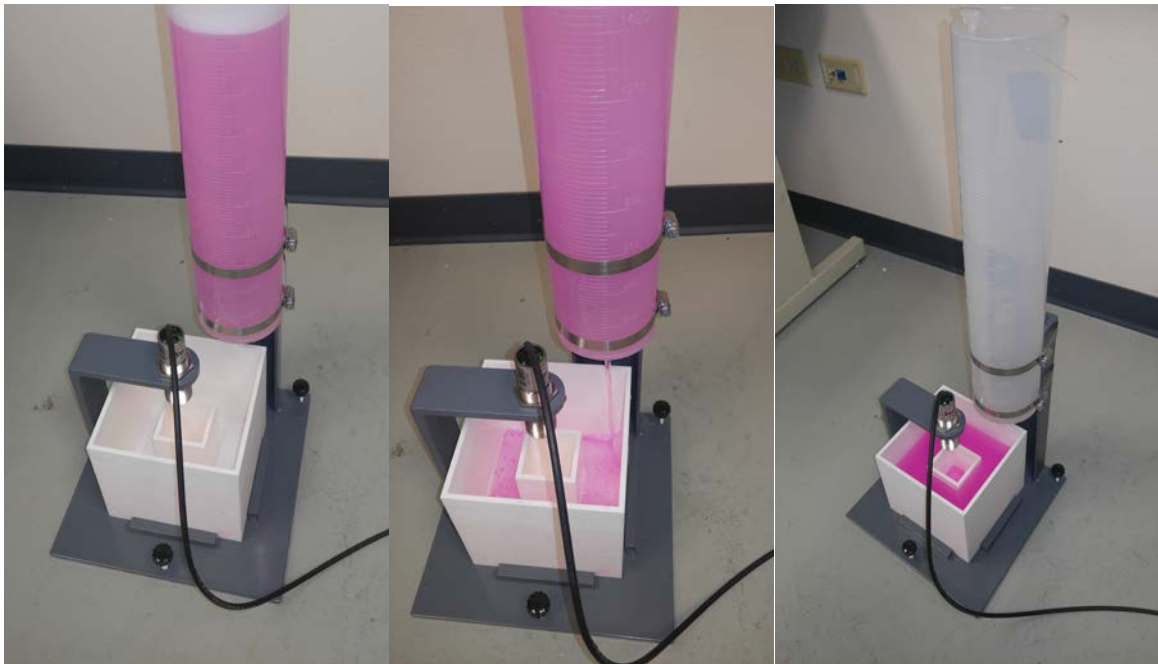


Figure 18. Custom validation experiment photos.

Surface tension effects will also be considered in this experiment. A series of tests will be repeated with and without the addition of a small amount of soap to the water to assess the surface tension effects. It is uncertain how the SPH codes will account for the surface tension, so both cases will be modeled and compared. Tests without soap in the water were performed in May 2016. The tests with soap are being refined to ensure that there is enough soap in the water to reduce the surface tension without resulting in the formation of foam as the water falls into the box. Figure 19 shows the depth measurements recorded on May 20th 2016. Five tests were performed, using 2100 ml of water in the cylinder. The graph shows how closely all of the tests performed, with the sensor beginning to measure flow into the center volume at around 60 seconds into the experiment, then beginning to level out after about 90 seconds. The overall height measured at the end of each test are within 0.25 cm of 4 cm.

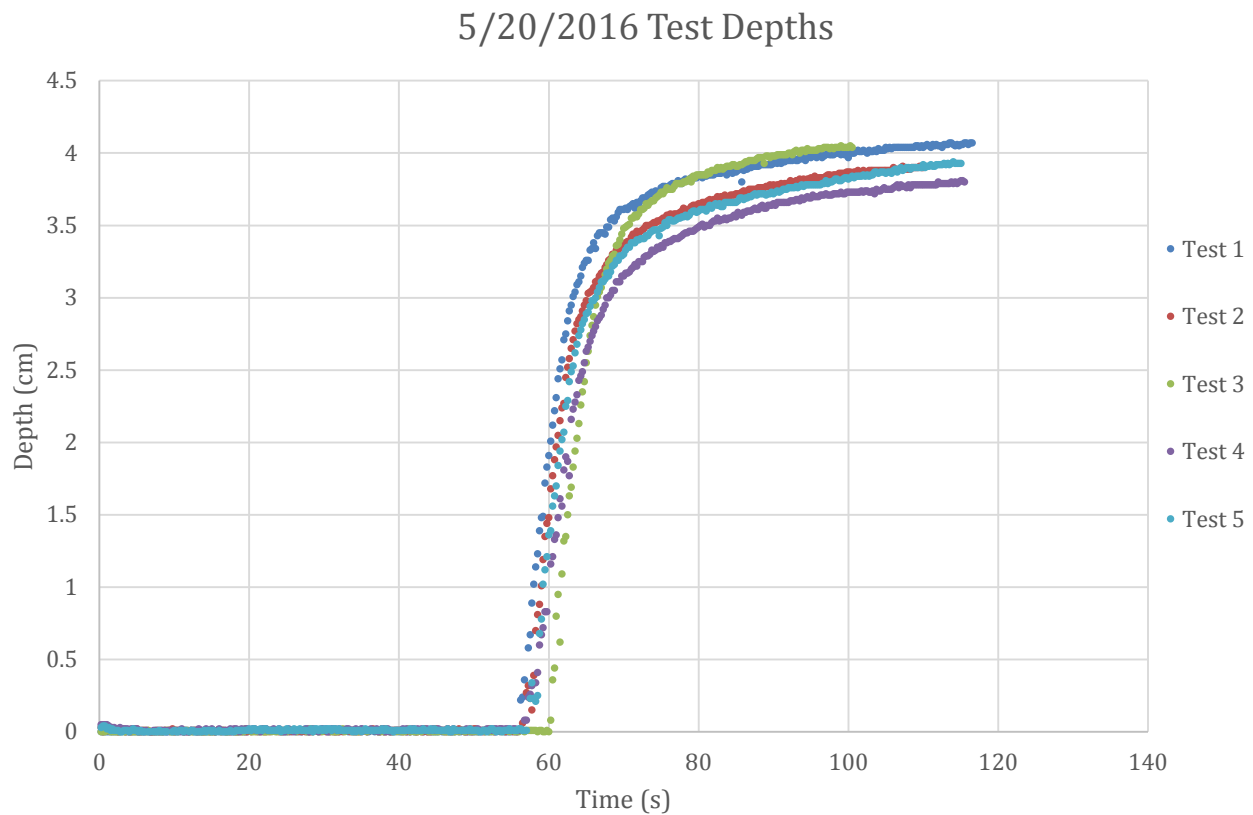


Figure 19. Validation experiment measurements.

The analytical solution work has been started but there are no results yet to report. The modeling phase of this has not been started yet, and will likely wait until August. The current goal of this project for the summer is to finish collecting data from the experiments and to finish the analytic solution.

4.2 Flow Over Ogee Spillway Validation

An existing CFD validation case involving flow over an ogee spillway will also be used for SPH code validation. An ogee spillway is a hydraulic structure used in a variety of situations. Figure 20 shows an ogee spillway with dimensions and flow parameters.

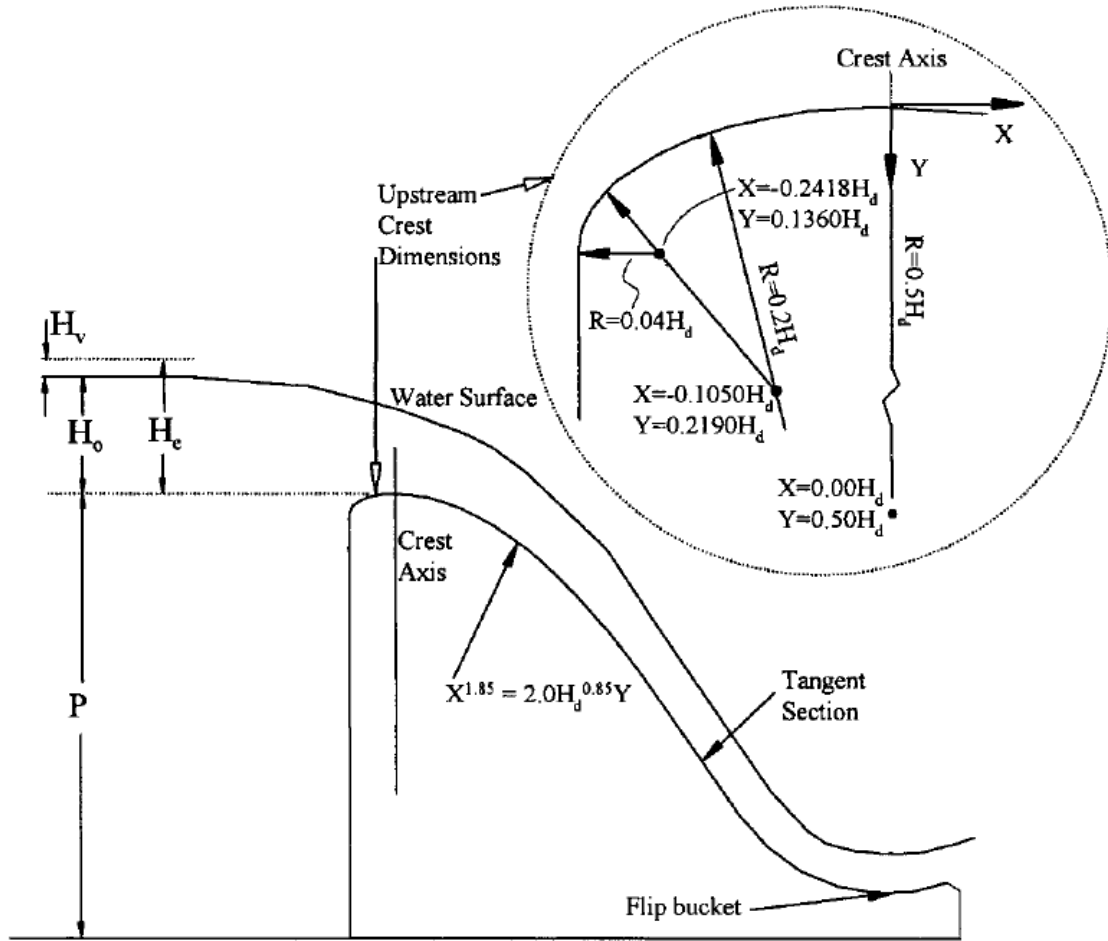


Figure 20. Ogee dimensions and flow parameters.

Since an ogee spillway is a commonly used structure, it should be known if SPH can accurately model flow over such a structure. Data for flow over an ogee spillway that will be used for SPH validation is available.⁵ The data includes physical data from an experiment, performance data from U.S. Bureau of Reclamation and U.S. Army Corps of Engineers, and numerical data from a CFD simulation. The results from the SPH simulation will be compared to the results from the above to determine how accurate SPH models flow over an ogee spillway.

Before the comparison can be made, an SPH model needs to be created. One of the issues with flow over a spillway is that a constant supply of water needs to exist. Therefore, an SPH code particle emitter is needed to create the simulation. Out of the four codes that were chosen for further research, only one code has a known particle emitter, which is Neutrino. DualSPHysics does not have a particle emitter in its current version, but the developers plan on adding one in their next version. As for GPUSPH and LAMMPS, more research will need to be done if there is an existing particle emitter in these codes or if there are plans to add one. However, it should be known that this validation can be used for the other codes if or when they get a particle emitter. Since Neutrino has a known particle emitter, this is the code that will be used to conduct the spillway validation.

⁵ B. M. Savage and M. C. Johnson, "Flow over Ogee Spillway: Physical and Numerical Model Case Study," *Journal of Hydraulic Engineering*, pp. 640-649, 2001.

The next step was to start creating a model of the spillway setup. An example of an ogee spillway was prepared so that modeling could begin. However, the exact model of the system will be obtained to complete the actual validation. The rough model consists of the spillway, a box, which acts as the flume, and a particle emitter. The dimensions of the rough model are just used to determine how to create the flow over the spillway. Two different techniques were tried to create the flow over the spillway: have the flow going horizontally towards the spillway and have the flow coming from the bottom. Figure 21 and Figure 22 show the two different setups for the particle emitter in Neutrino.

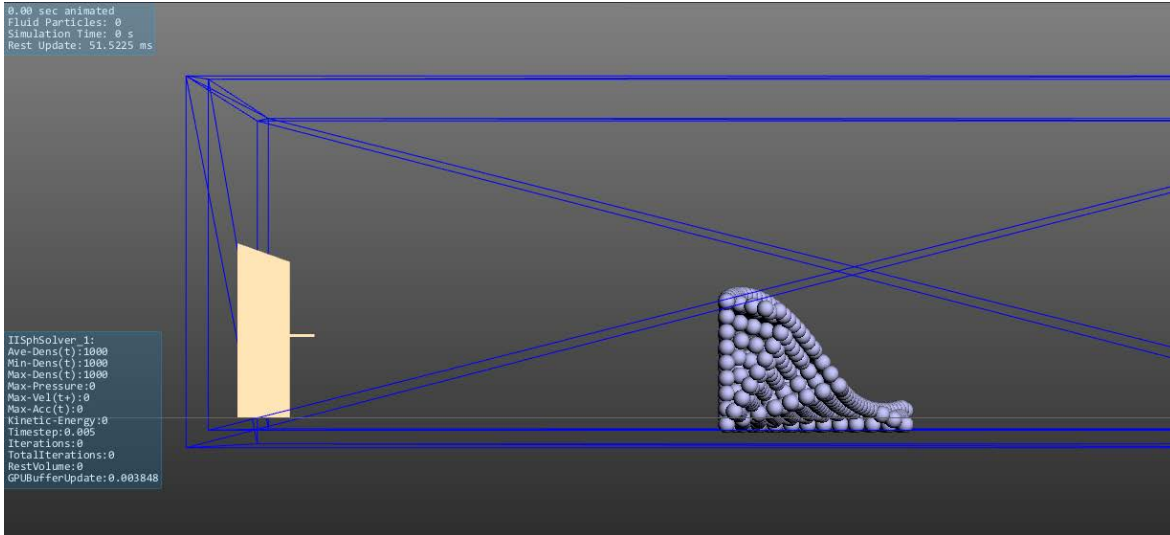


Figure 21. Horizontal flow particle emitter setup.

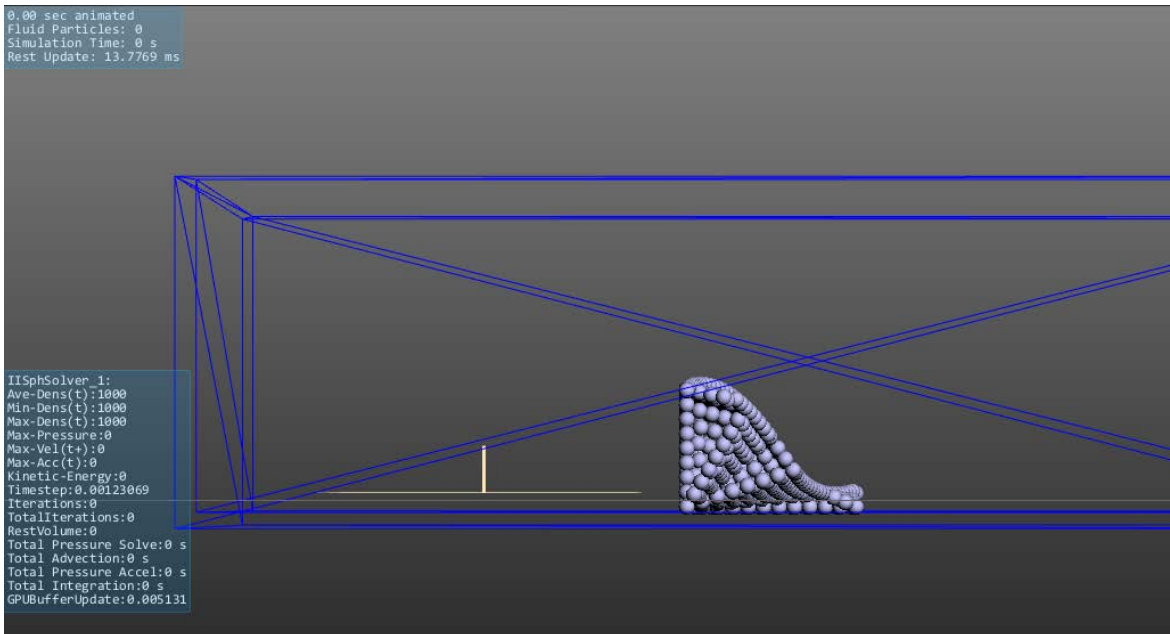


Figure 22. Bottom particle emitter setup.

The two techniques were then examined to determine how each one worked. The first technique that was modeled was the horizontal technique. At the beginning of this technique, the particles hit the spillway and cause a wave in the opposite direction. The wave does eventually settle out as shown in Figure 23 through Figure 25.

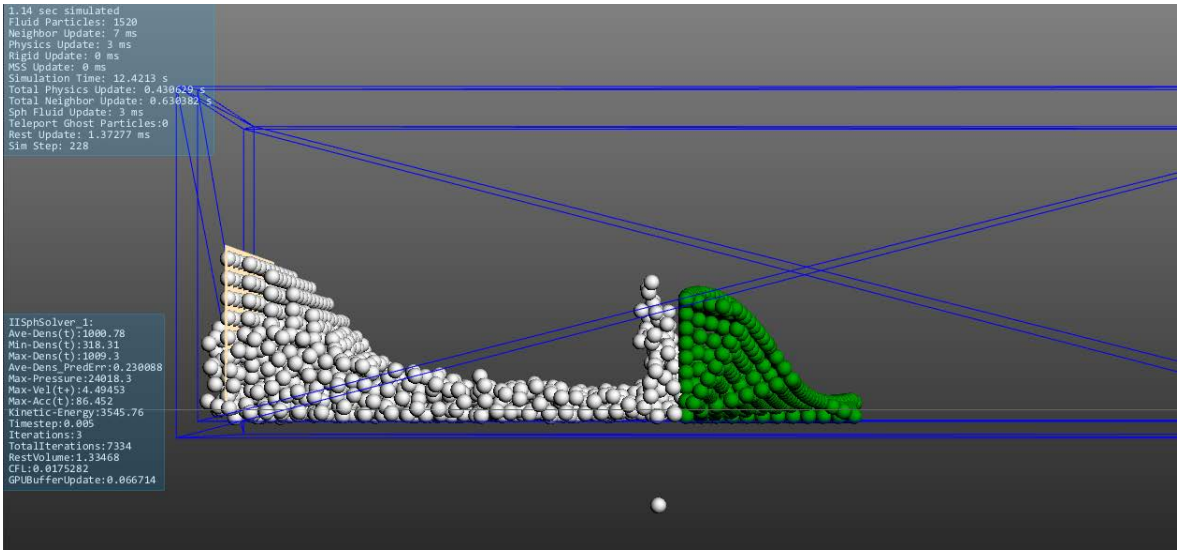


Figure 23. Horizontal particle emitter wave beginning.

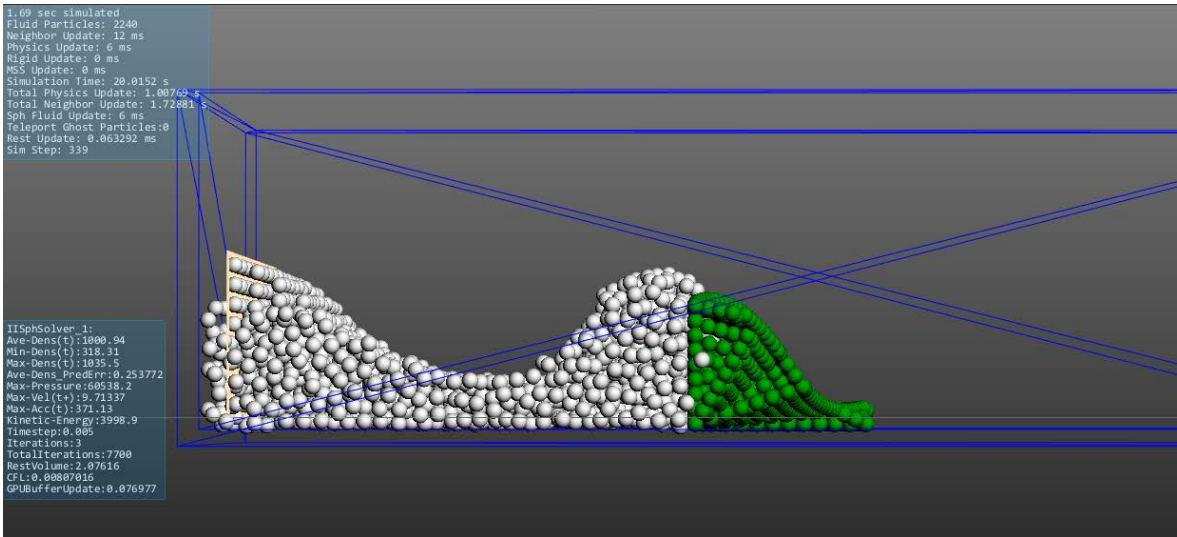


Figure 24. Horizontal particle emitter wave.

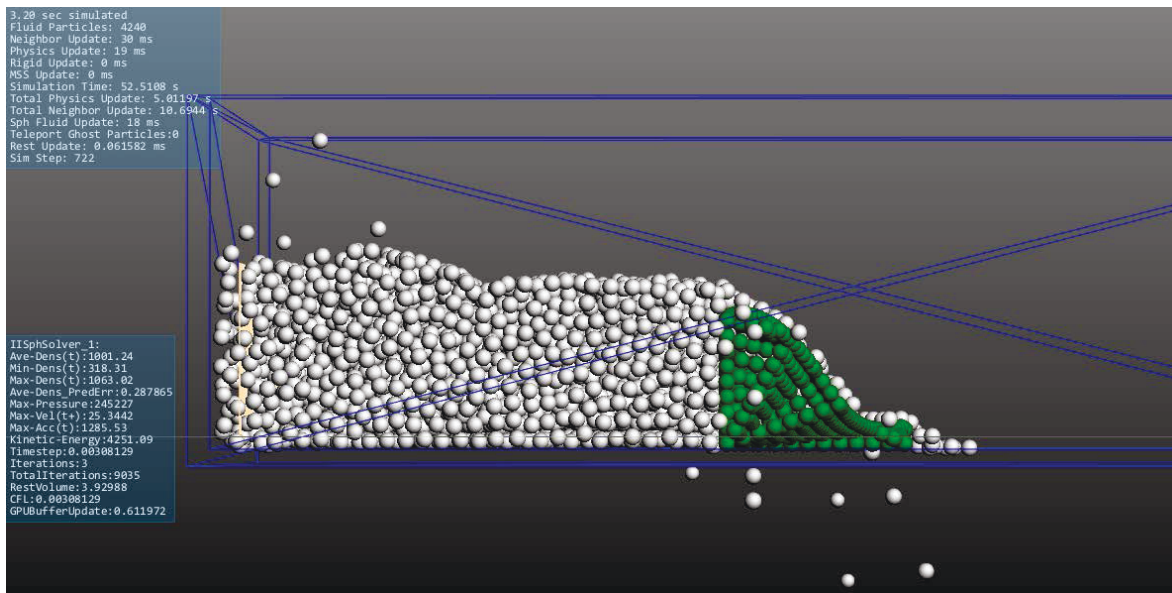


Figure 25. Horizontal particle emitter wave settled out.

After the wave settles out and the particles have filled the area behind the spillway, the particles close to the particle emitter will begin to splash up. Another anomaly that occurs is that particles will go through the dam and bottom of the box by the spillway. Both of these are shown in Figure 26.

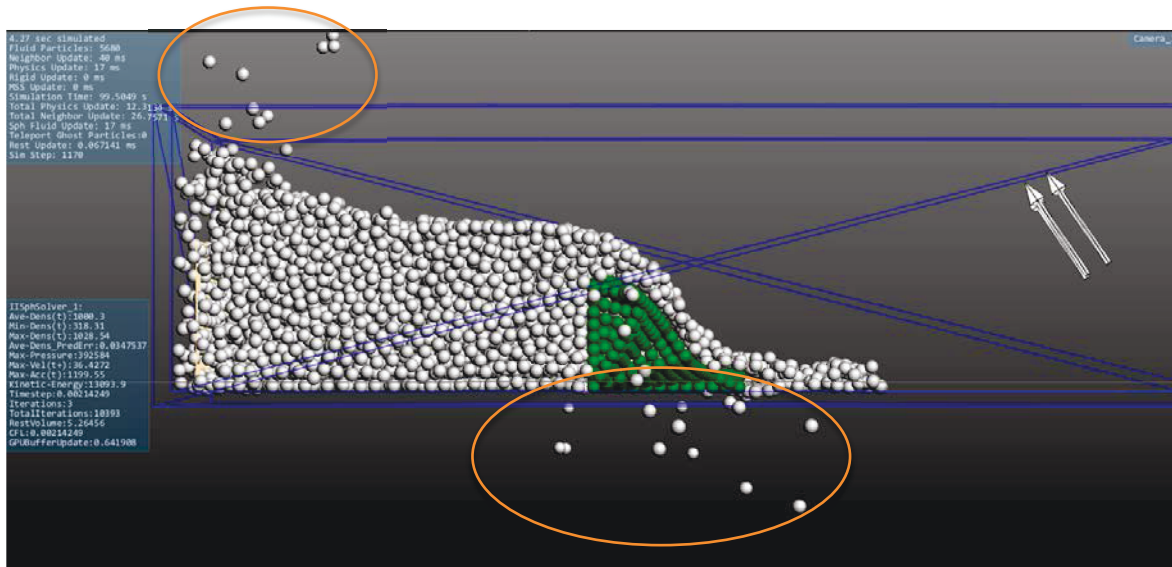


Figure 26. Splashing particles and emitted particles.

The next technique that was used was a particle emitter at the bottom of the box. By having the particle emitter at the bottom, it removed the wave that the horizontal particle emitter created. Figure 27 shows the bottom particle emitter and that no wave is created.

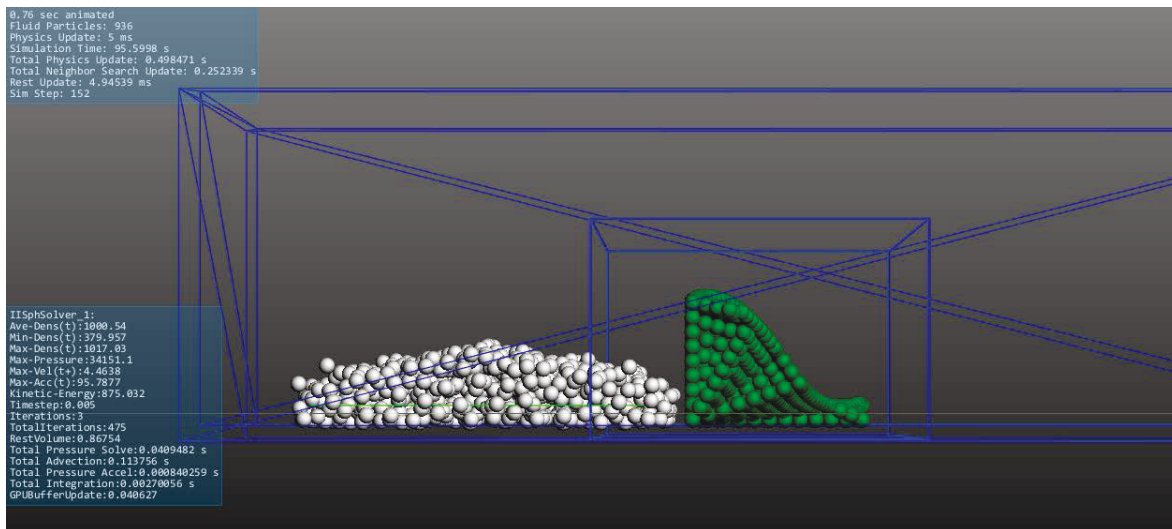


Figure 27. Bottom particle emitter beginning.

The bottom particle emitter also removed the splashing particles. However, some particles are still going through the bottom of the box, which is shown in Figure 28.

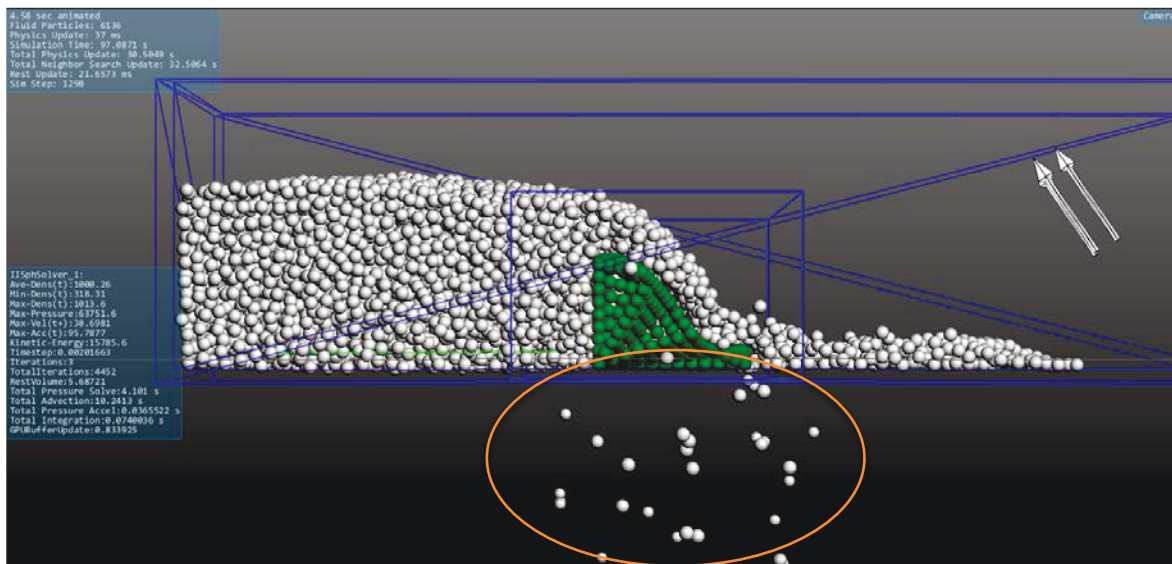


Figure 28. Bottom particle emitter with emitted particles.

At this point, the best technique for emitting the particles is using the bottom particle emitter, but the data for this technique must be validated to determine if this is a reasonable way of modeling it. If the data for the bottom particle emitter does not give similar results, a combination of the bottom emitter and horizontal emitter might need to be analyzed. As for the particles being emitted through the box, this is a known boundary condition issue in Neutrino. For the exact model, the emission of these particles will try to be minimized, but otherwise will have to be ignored until a fix is in place.

Once the model creation is finalized, the measurements that are required needed to be known. The available data from the experiment and CFD model include flow rates, elevation heads, and pressure heads on the spillway. Therefore, the same must be obtained for the SPH model. The results, in the footnoted paper by Savage and Johnson, included plots of non-dimensional flow rate vs. non-dimensional elevation head, relative

percent error vs. non-dimensional elevation head, non-dimensional pressure head vs. position, and absolute pressure difference vs. position. Figure 29 shows the pressure tap locations where the pressure heads are measured and Figure 30 through Figure 33 show the results. These figures appeared in the footnoted paper by Savage and Johnson.

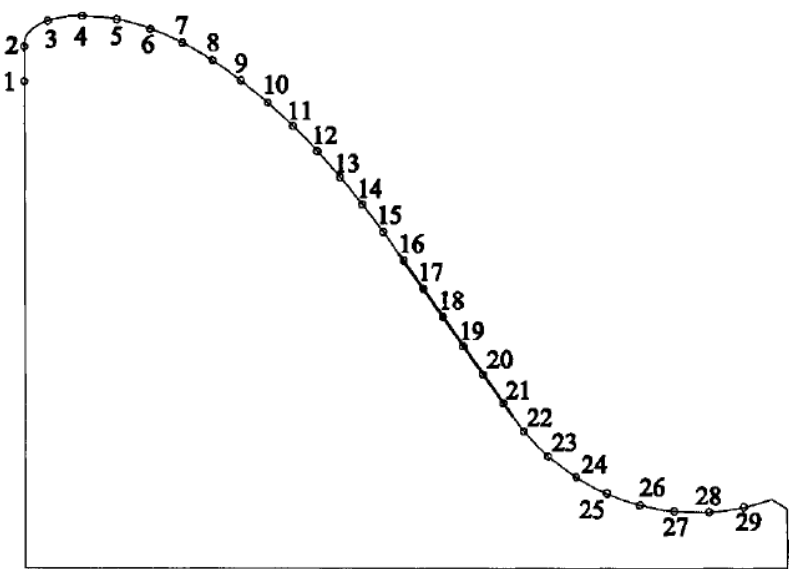


Figure 29. Pressure tap locations.

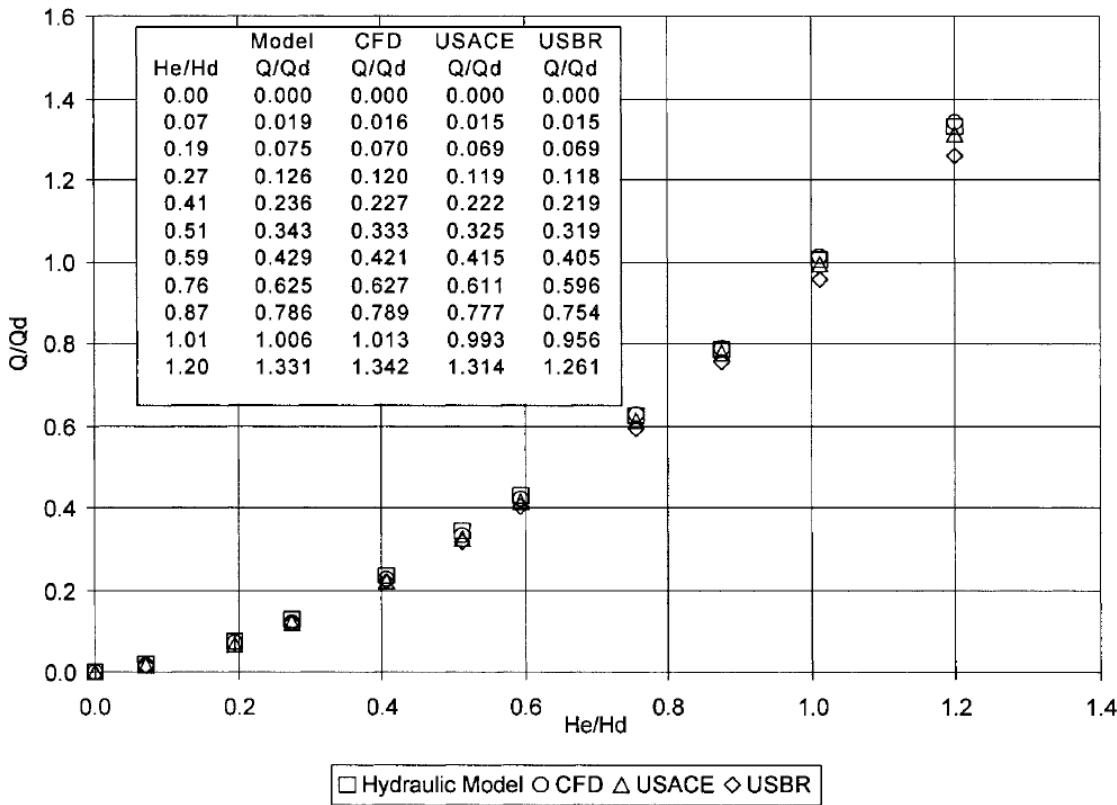


Figure 30. Normalized discharge comparison.

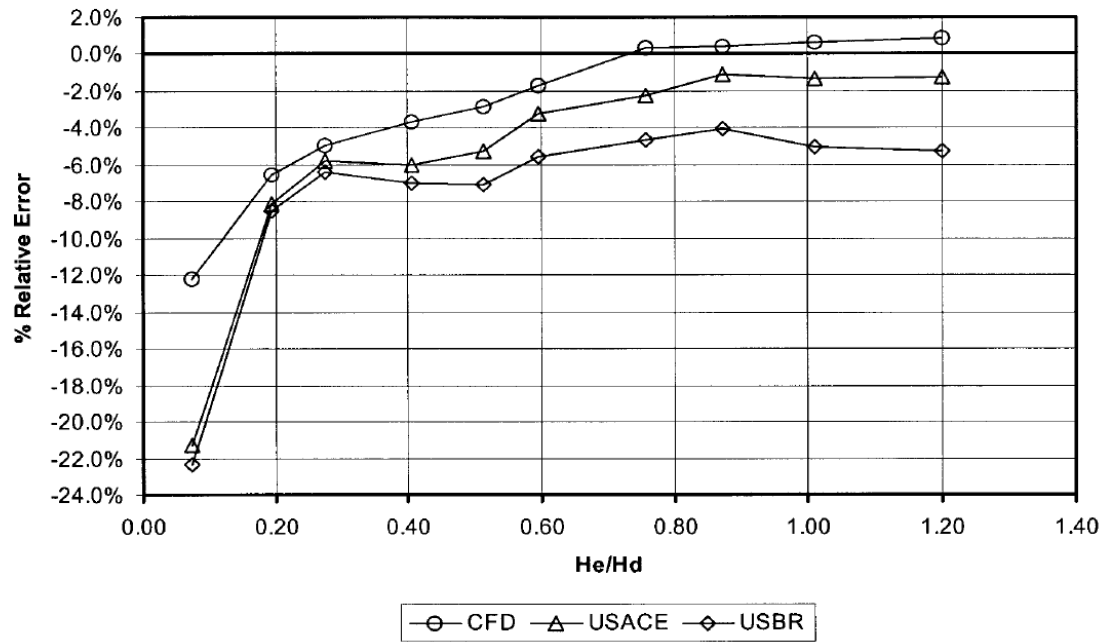


Figure 31. Relative percent error in discharge using physical model as basis.

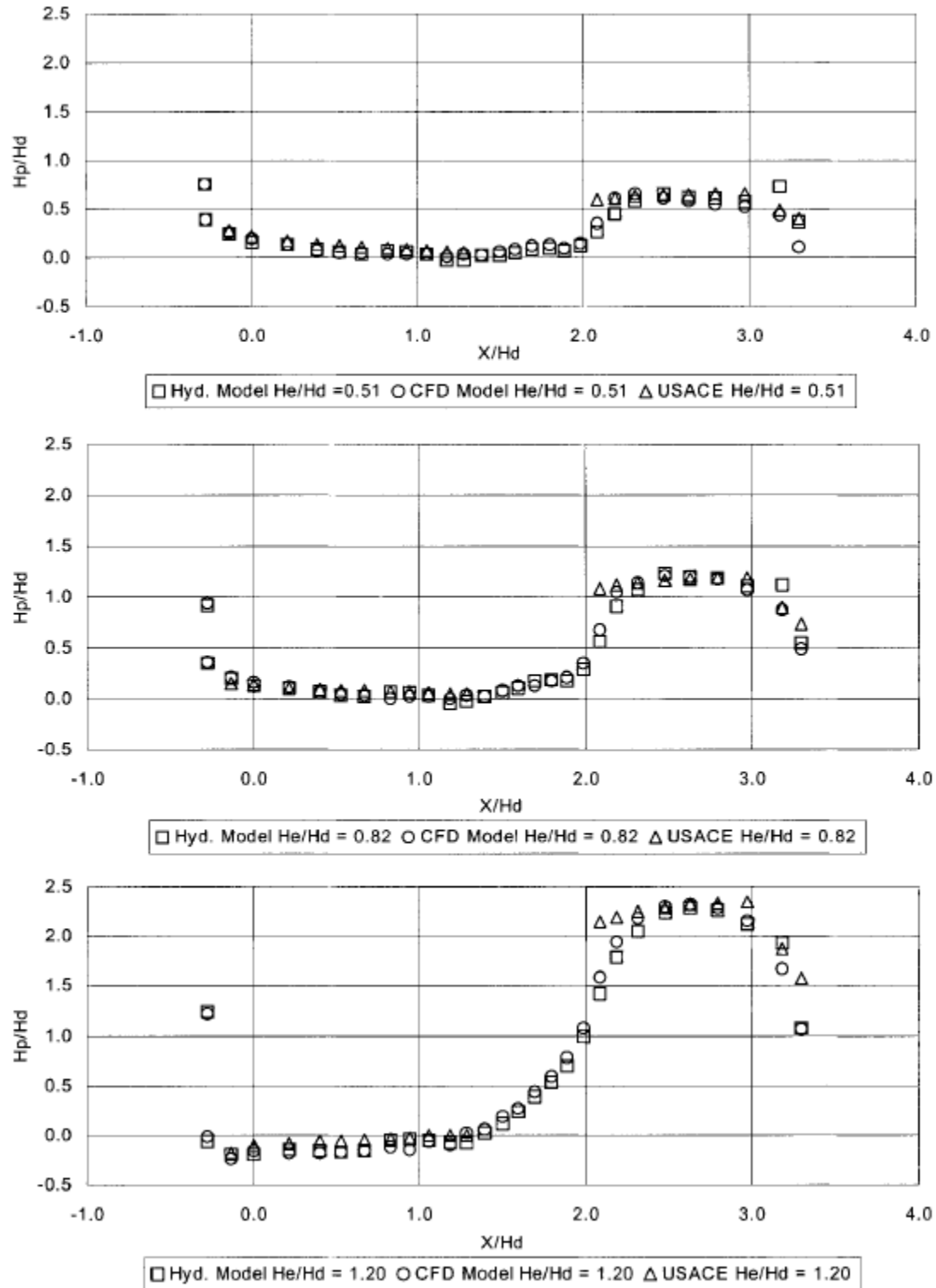


Figure 32. Crest pressure comparison.

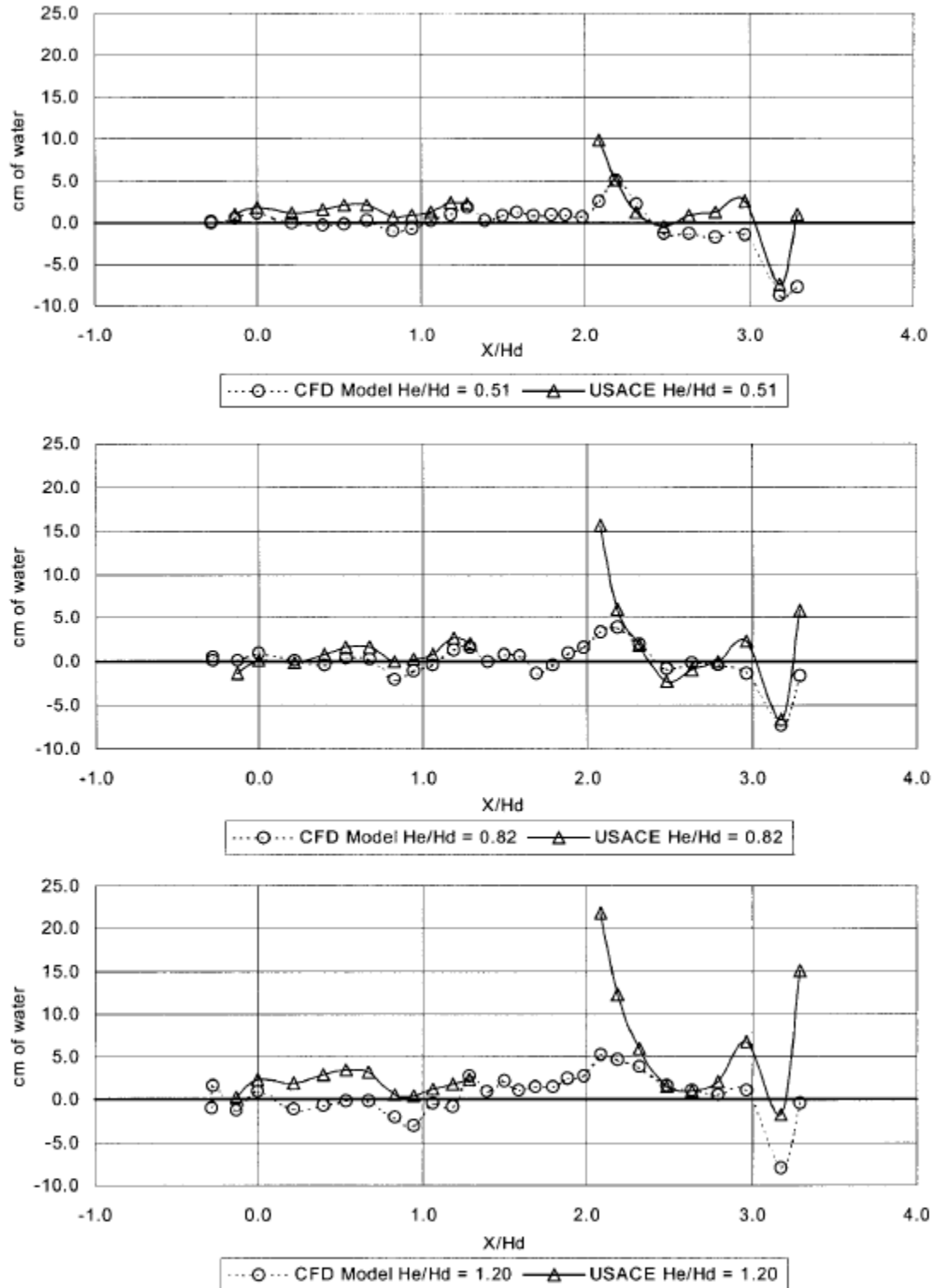


Figure 33. Absolute pressure difference using physical model as baseline.

Based on the above reported results, the next step was to determine how to get the appropriate measurements in order to compare the data from the SPH simulation to the results in the paper. The first measurement to determine is the elevation head. In Figure 20, it shows the elevation head as H_e . However, the

elevation head also includes the velocity head. Therefore, to determine the proper elevation head, Equation 3 must be used.

$$H_e = H_o + \frac{v^2}{2g} \quad (3)$$

This equation uses the elevation above the spillway, H_o , the velocity of the water in the horizontal direction, v , and the gravitational acceleration to determine the elevation head. All of these parameters can either be measured or set in Neutrino. Therefore, the elevation head can be calculated.

As for the flow rate, the flow rate will be determined based on the size and velocity of the particle emitter. Lastly, the pressure head will be determined by measuring the pressure at different locations on the spillway in Neutrino. Once the pressure is known, the pressure head can be determined using Equation 4.

$$H_p = \frac{P}{\rho g} \quad (4)$$

As for the errors, the relative percent error for the discharge is determined using Equation 5 and the absolute pressure different is determined using Equation 6.

$$\% \text{ relative error} = \frac{Q_{SPH} - Q_{physical}}{Q_{physical}} * 100\% \quad (5)$$

$$\Delta P = H_{SPH-pressure} - H_{physical-pressure} \quad (6)$$

With all of the information above as well as measurements from Neutrino, all of the required data should be able to be obtained to compare the SPH results to the paper results which will result in a validation model for SPH.

Since the validation cases for the SPH codes are known, the next step is to conduct the validation. This consists of simulating the custom experiment and flow over an ogee spillway in the different codes and comparing the data. The data comparison will determine how realistic the results are for each of the SPH codes and what codes should continue to be investigated. For the codes that make it past validation, the next step will be to look into the source code. The reason for looking at the source code is because the code will need to be modified in order to obtain the goal of incorporating flooding failure analysis. Once the modification step is reached, a more specific plan of attack will be developed. The final step will be to select one or more codes to incorporate component flooding failure analysis. The chosen code or codes will then be modified so that a user can model a building or location that is of concern of flooding. After the location is modeled, the user could select what type of flooding is to be simulated, rising, spray, or wave, and the details of the event, flow rate, wave height, etc....

After the model is finalized, the user can then run the code. The code will have flooding failure models for the different components that are in the model. The component failure models will come from CFEL. As the code runs, it will be able to tell when certain components have failed. It will then inform the user at what time in the simulation that the specific component has failed. The code will also be able to adapt as components fail. For example, if a door fails, water will then enter the area that is behind the door. Once the code is done running, the user will then be able to visualize the simulation with failed components changing color as they fail. A more detailed approach on the specifics of developing this code will be specified once a code or codes have been selected.

5. FULL SCALE COMPONENT TESTING

The ultimate CFEL goal is testing actual NPP components. In order to cover the full spectrum of components; electrical, mechanical, and structural components will require testing. While doorways are a simple and common feature in NPPs, they play a significant role in determining the overall risk. For example, Figure 34 shows an example of a doorway flooding damage situation encountered in the Fukushima tsunami event. Doorways provide a point of access for water to enter a room and can fail as a protective barrier. In a literature review of US NPP flooding events, a number of flooding events arose from water leaking underneath or forcing through inadequately secure doors. The end result often being the submerging or damaging of vulnerable components located within.



Figure 34. Door failure in the Fukushima nuclear power plant.

Small scale testing has already shown significant value in understanding how doors fail. While the CFEL design and construction progresses, an existing water reservoir will be used in conjunction with a new above grade testing tank to test full scale doors and other components. The new tank was built to test full scale doors and other components in a water rise scenario. After having a deep level of understanding of the reliability of the interior doors, the testing will move forward to the exterior doors. The test will provide data to be used in developing reliability models. The general arrangement of the experiment design is shown in Figure 35.

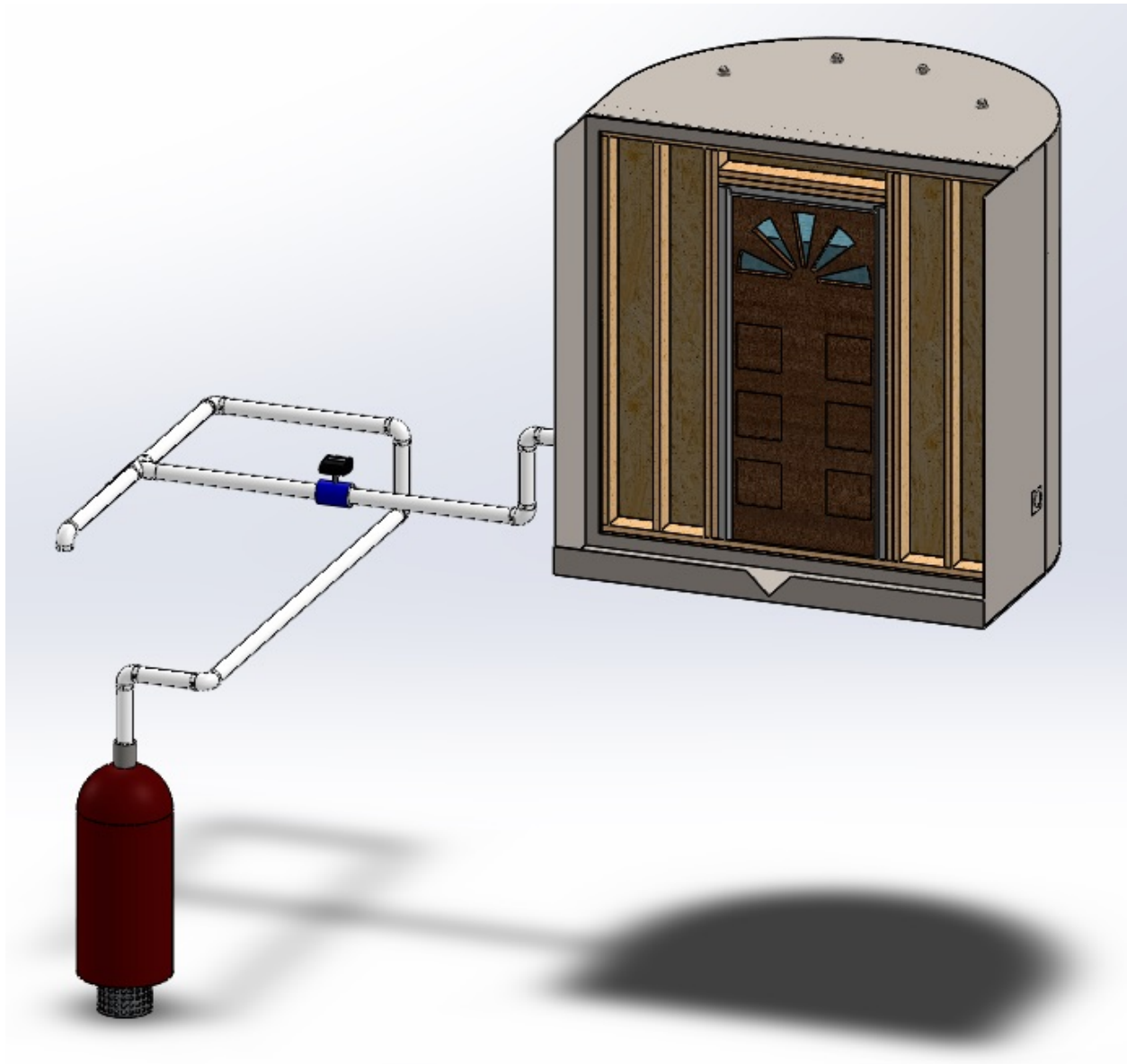


Figure 35. Full-scale testing arrangement.

The 8-foot-tall tank, shown in Figure 36, was designed, built, and delivered in May, 2016. The tank is connected to the existing 8000-gallon water reservoir using PVC pipe and a 5-hp pump. The testing tank can hold up to 2000 gallons of water. The tank can be pressurized if needed to simulate a water depth greater than the height of the door. The 5-hp pump, piping, electromagnetic flow meter, have been installed and are functional. A pressure relieve valve, air relive valve, and pressure gauge was also installed on the top of the tank as can be seen in Figure 37.



Figure 36. Full-scale testing tank.



Figure 37. Testing tank pressure relief valve, air vent, and pressure gauge.

For the initial test, a 3-foot-wide interior door was selected, see Figure 38. The door frame was built on standard code. The vertical studs were placed 9 inches apart and two base studs were used to place the door. Currently, the full scale door test team is working on instrumentation and data acquisition equipment. Testing of the interior door is expected to occur in early July.



Figure 38. Interior door installed in testing tank.

Future tests will utilize several types of doors. The two types of doors that are of immediate interest are industrial steel doors, and roll up doors. The steel doors of interest are both single and double doors. It is expected that the reliability of these doors will be much higher than the interior to be used in the initial test. Figure 39 shows an example of the steel door that would be used for a single steel door test. This door is 36" x 80", which would fit within the tank.



Figure 39. Steel door example

Roll-up doors offer more variation in sizes. A likely dimension for the door would be 7 feet tall by 6 feet wide, in order to make it fit in the tank, but still be large enough to mimic a roll up door in an NPP. Nuclear plants can have much larger roll up doors than this depending on the place and use, but testing these large of doors is not possible with the current facilities. Figure 40 shows an example of the type of roll up door that will be tested.



Figure 40. Roll-Up door example.

6. CONCLUSION

Research work in the area of NPP component reliability under flooding conditions is progressing. The work includes; CFEL water rise and water spray design work, wave impact research, SPH modeling and validation experiments, and full-scale component testing. Work is continuing on the development of the CFEL Users Guide which will document the capabilities developed to date from Phase 1 and Phase 2 installation projects as well as the lessons learned and methodologies. The guide will serve as an important asset to communicating the CFEL capabilities to stakeholders, as well as guiding the planning, preparation, and execution of larger scale experiments.

Finally, communications with industry representatives have begun to help identify components that merit testing as well as to guide research activities. Discussions have been held with representatives from Energy Northwest which operates the Columbia Generating Station in Washington state as well as Exelon Corporation which operates a fleet of NPPs in the mid-west and north-east. The discussions are in their initial stages and have included the possibility of acquiring non-radioactive components that are considered to be excess.